

Authors' response to the editor review on "A process-based model for ammonia emission from urine patches, GAG (Generation of Ammonia from Grazing): description, validation and sensitivity analysis"

We thank the editor for the comments. Our responses and the changes we make to address the editor's suggestions are provided below point-by-point. This is followed by an updated version of the manuscript and the supplementary material, in which we marked all the modifications we carried out following the reviewers' and the editors comments.

We would like to ask the editor to link our paper to the ÉCLAIRE Special Edition of the journal.

Comment 1: *One reviewer pointed out that the present comparison with the measurements of Laubach et al. (2012) represents rather a model calibration than a "model validation". Need the authors change the text (including the abstract) based on this?*

Our response: In our response to the reviewers (to Reviewer#2 in Comment 3; to Reviewer#3 in Comment 35) we explained that our choice of the thickness of the emission layer (Δz) was arbitrary based on the literature, and we defined the buffering capacity (β) during test simulations. To get a wider picture of how the modelled NH_3 emissions are affected by the uncertainty of these parameters, we carried out a comprehensive sensitivity analysis to Δz and β in Section 5.2 and 5.3, respectively.

In regard of especially the buffering capacity, we accept the editor's point that the work we have done was not clearly a model validation. However, we believe that it is not a better description to call this a "model calibration". We think that a comprehensive model calibration should involve a statistical analysis during which the unknown parameters are defined by minimizing the difference between the measured and modelled variables. We clearly did not take such an approach.

As a compromise, we replace the word "validation" with "test simulation" or "model test" as appropriate in the text. Please see the detailed list of corrections below. (We present the complete modified abstract in our response to Comment 2.)

Change to the manuscript:

We change the title to: "A process-based model for ammonia emission from urine patches, GAG (Generation of Ammonia from Grazing): description and sensitivity analysis."

On page 10065 in line 4 we change "from the model validation" to "from the test simulation"

On page 10077 in line 7 we change "for the validation site of the present study" to "for the site whose measurement we used in the test simulation".

We change the title of Section 3 (page 10081) to: "Measurement data used in the test simulation".

On page 10081 in line 3 we change "for validation we chose" to "for testing the model we chose".

On page 10081 in line 23 we change "We validated our model results against measurements" to "We compared our model results with measurements".

On page 10082 from line 6 we change "...as well as validation data together with their modification..." to "...as well as the measurement data we used to compare our model results, together with their modification...".

On page 10082 in line 13 we change "To validate the simulation of θ " to "To compare θ with the observations".

We change the title of Section 4 (page 10082) to: "Test simulation".

On page 10082 in line 18 we change "The results of the model validation" to "The results of the test simulation".

On page 10085 in line 25 we change "at the validation site" to "at the measurement site".

On page 10091 in line 9 we change "In the validation experiment" to "In the test simulation".

On page 10092 in line 1 we remove the sentence "According to the model validation, these are well represented by the model."

In the caption of Table 2 (page 10100) we change "Input and validation data for testing the model" to "Measured data used as input and the base of comparison with the model results".

In Table 2 (page 10100) we change "Validation data" to "Data used in the comparison".

In the caption of Table 3 (page 10101) we change "Model validation statistics" to "Statistics calculated for the comparison of the modelled and measured variables".

In the caption of Figure 2 (page 10105) we change "results that were validated in this study" to "results that were compared with measurements".

We remove from Figure 2 (page 10105) "validated in this study".

Comment 2: *The abstract should be prepared just in one paragraph and better more concisely.*

Our response: Please see the shortened (to one paragraph, and 213 words instead of the original 339), modified abstract below.

Change to manuscript:

We change the whole abstract to the following paragraph:

"In this paper a new process-based, weather-driven model for ammonia (NH₃) emission from a urine patch has been developed and its sensitivity to various factors assessed. The GAG model (Generation of Ammonia from Grazing) is capable of simulating the TAN (total ammoniacal nitrogen) and the water content of the soil under a urine patch and also soil pH dynamics. The model tests suggest that ammonia volatilization from a urine patch can be affected by the possible restart of urea hydrolysis after a rain event as well as CO₂ emission from the soil. The vital role of temperature in NH₃ exchange is supported by our model results; however, the GAG model provides only a modest overall temperature dependence in total NH₃ emission compared with the literature. This, according to our findings, can be explained by the higher sensitivity to temperature close to urine application than in the later stages and may depend on interactions with other nitrogen cycling processes. In addition, we found that wind speed and relative humidity are also significant influencing factors. Considering that all the input parameters can be obtained for larger scales, GAG is potentially suitable for field and regional scale application,

serving as a tool for further investigation of the effects of climate change on ammonia emissions and deposition.”

1 **A process-based model for ammonia emission from urine**
2 **patches, GAG (Generation of Ammonia from Grazing):**
3 **description, validation and sensitivity analysis**

4
5 **A. Móríng^{1,2,3}, M. Vieno^{1,2}, R.M. Doherty¹, J. Laubach⁴, A. Taghizadeh-Toosi⁵, M.**
6 **A. Sutton²**

7 [1]{University of Edinburgh, Crew Building, Alexander Crum Brown Road, Edinburgh, EH9
8 3FF}

9 [2]{NERC, Centre for Ecology & Hydrology, Edinburgh, Bush Estate, Midlothian, Penicuik,
10 EH26 0QB}

11 [3]{Hungarian Meteorological Service, Kitaibel P. u. 1, H-1024 Budapest, Hungary}

12 [4]{Landcare Research, P.O. Box 69040, Lincoln 7640, New Zealand}

13 [5]{Department of Agroecology, Aarhus University, Blichers Allé 20, DK-8830 Tjele,
14 Denmark}

15 Correspondence to: A. Móríng (A.Moring@sms.ed.ac.uk)

16
17 **Abstract**

18 In this paper a new process-based, weather-driven model for ammonia (NH₃) emission from a
19 urine patch has been developed and its sensitivity to various factors assessed. ~~This model, the~~
20 ~~GAG model (Generation of Ammonia from Grazing) was developed as a part of a suite of~~
21 ~~weather driven NH₃ exchange models, as a necessary basis for assessing the effects of climate~~
22 ~~change on NH₃ related atmospheric processes~~The GAG model (Generation of Ammonia from
23 Grazing) is capable of simulating the TAN (total ammoniacal nitrogen) and the water content
24 of the soil under a urine patch and also soil pH dynamics. The model tests suggest that ammonia
25 volatilization from a urine patch can be affected by the possible restart of urea hydrolysis after
26 a rain event as well as CO₂ emission from the soil. The vital role of temperature in NH₃
27 exchange is supported by our model results; however, the GAG model provides only a modest
28 overall temperature dependence in total NH₃ emission compared with the literature. This,

1 according to our findings, can be explained by the higher sensitivity to temperature close to
2 urine application than in the later stages and may depend on interactions with other nitrogen
3 cycling processes. In addition, we found that wind speed and relative humidity are also
4 significant influencing factors. Considering that all the input parameters can be obtained for
5 larger scales, GAG is potentially suitable for field and regional scale application, serving as a
6 tool for further investigation of the effects of climate change on ammonia emissions and
7 deposition.

8 ~~GAG is capable of simulating the TAN (Total Ammoniacal Nitrogen) content, pH and the water~~
9 ~~content of the soil under a urine patch. To calculate the TAN budget, GAG takes into account~~
10 ~~urea hydrolysis as a TAN input and NH₃ volatilization as a loss. In the water budget, in addition~~
11 ~~to the water content of urine, precipitation and evaporation are also considered. In the pH~~
12 ~~module we assumed that the main regulating processes are the dissociation and dissolution~~
13 ~~equilibria related to the two products of urea hydrolysis: ammonium and bicarbonate. Finally,~~
14 ~~in the NH₃ exchange flux calculation we adapted a canopy compensation point model that~~
15 ~~accounts for exchange with soil pores and stomata as well as deposition to the leaf surface.~~

16 ~~We validated our model against measurements, and carried out a sensitivity analysis. The~~
17 ~~validation showed that the simulated parameters (NH₃ exchange flux, soil pH, TAN budget and~~
18 ~~water budget) are well captured by the model ($r > 0.5$ for every parameter at $p < 0.01$ significance~~
19 ~~level). We found that process based modelling of pH is necessary to reproduce the temporal~~
20 ~~development of NH₃ emission. In addition, our results suggested that more sophisticated~~
21 ~~simulation of CO₂ emission in the model could potentially improve the modelling of pH.~~

22 ~~The sensitivity analysis highlighted the vital role of temperature in NH₃ exchange; however,~~
23 ~~presumably due to the TAN limitation, the GAG model currently provides only a modest overall~~
24 ~~temperature dependence in total NH₃ emission compared with the values in the literature.~~

25 ~~Since all the input parameters can be obtained for study at larger scales, GAG is potentially~~
26 ~~suitable for larger scale application, such as in regional atmospheric and ecosystem models.~~

28 **1 Introduction**

29 The consequences of strong emission of reactive nitrogen compounds (N_r), dominated by the
30 emission of ammonia (NH₃), are widely discussed: threatening air, water and soil quality, it
31 endangers also ecosystems as well as human health in many ways (Sutton et al., 2011, Galloway

1 et al., 2008, Fowler et al., 2013). Globally 70% of NH₃ released to atmosphere originates from
2 agricultural sources, such as livestock housing, manure management and fertilizer spreading on
3 fields (EDGAR, 2011). According to the latest available report of the UK government agency
4 DEFRA (Department for Environment Food and Rural Affairs), in the UK grazing accounts for
5 ca. 11% of the total NH₃ emission (Misselbrook et al., 2012). ~~In spite of its small~~ Although this
6 proportion of in the total national emission is rather small, since two thirds of the grasslands are
7 estimated to be grazed (Hellsten et al., 2008), NH₃ emission from grazing affects a significant
8 percentage of the country.

9 ~~Ammonia exchange between atmosphere and surface, as it was confirmed~~ As demonstrated by
10 both laboratory and field experiments (Farquhar et al., 1980; Sutton et al., 1995), ammonia
11 exchange between atmosphere and surface is a bidirectional process and dependent largely on
12 meteorological factors, especially temperature. The direction of the net NH₃ exchange at any
13 time depends on the relative magnitude of the ambient air concentration of NH₃ high above the
14 surface and the concentration of NH₃ right above the surface (referred to as the ‘compensation
15 point’). If the air concentration is the larger of the two, deposition occurs; whilst in the opposite
16 case, emission takes place.

17 During grazing, the dominant NH₃ source is urine, rather than dung (Petersen et al., 1998,
18 Laubach et al., 2013). In a urine patch ammonium (NH₄⁺) is produced by urea hydrolysis. ~~The~~
19 ~~process is catalysed by~~ Because of the enzyme urease, which is the product of several bacteria
20 species, in the presence of water. To maintain the chemical equilibria equilibrium between NH₄⁺
21 and ~~dissolved as well as gaseous~~ NH₃, production of increasing NH₄⁺ concentration results in
22 an NH₃ by ureolysis is accompanied by NH₃ release from the urine solution to the gas phase.
23 ~~This leads to a high~~ compensation point (that is usually higher than the ambient air
24 concentration) above the urine patch. ~~This~~ generally leading leads to NH₃ emission over from a
25 urine patch. According to the literature (e.g. Sherlock and Goh, 1985, Laubach et al., 2012 and
26 the references therein) the period with significant NH₃ emission lasts about 4-8 days after urine
27 deposition.

28 The state-of-the-art NH₃ exchange models for vegetated surfaces (e.g. Burkhardt et al., 2009,
29 Flechard et al., 2013), called canopy compensation point models, use the analogy of electrical
30 circuits. In these, electrical current and potential difference represent NH₃ fluxes and the
31 difference between the NH₃ concentrations at the different levels of the canopy, respectively.
32 The model resistances capture the influence of meteorological factors and the canopy on NH₃

Formatted: German (Germany)

1 transfer. The first ‘canopy compensation point’ model (Sutton et al., 1995) took into account
2 the net NH₃ exchange with vegetation (a single-layer model), considering exchange with
3 stomata and leaf surfaces. Later the canopy compensation point approach was developed by
4 including NH₃ exchange also with soil surface (a two-layer model by Nemitz et al., 2001) and
5 different parts of the plant, such as siliques and foliage (a three-layer model by Nemitz et al.,
6 2000).

7 An example for estimating emissions from an excretal source that applies a simple
8 compensation point model is the GUANO model (Riddick, 2012; Sutton et al., 2013), which
9 simulates the processes leading to NH₃ emission from seabird excreta. In this model the
10 compensation point is calculated based on Henry’s law (for ~~dissolution~~partitioning of NH₃) and
11 the dissociation of NH₄⁺ over a hypothetical surface covered by guano. In calculating the
12 compensation point, the effect of meteorological factors (temperature, wind speed, solar
13 radiation, relative humidity and precipitation) are represented, furthermore, it accounts for the
14 total ammoniacal nitrogen (TAN = NH₄⁺ + NH_{3(aq)}) budget on the surface simulating the
15 conversion of uric acid content of guano to ammoniacal nitrogen. In addition, it also calculates
16 the water budget on the surface using the Penman equation for evaporation.

17 Several attempts have been made to simulate NH₃ emission from urine patches as well as grazed
18 fields. Laubach et al. (2012) published an ~~inverse~~NH₃ volatilization model from urine patches
19 which was run in an “inverse” mode, to calculate soil resistance, applying also a simple
20 compensation point model. The equilibrium gaseous NH₃ concentration in the soil pores was
21 considered as a compensation point, and three resistances (a soil, an aerodynamic, and a quasi-
22 laminar resistance) were assumed between the soil and air concentration. Running the model in
23 ~~reverse~~predictive mode, simulating NH₃ emission, requires soil sampling and measurement of
24 pH and NH₄⁺ concentration of soil water.

25 The approach for the process ~~of~~ urea hydrolysis in the above mentioned ~~inverse~~model by
26 Laubach et al. (2012) is based on the earlier model of Sherlock and Goh (1985), which accounts
27 for the NH₃ volatilization from urine patches and aqueous urea. This model for describing the
28 transfer of NH₃ between surface and atmosphere operates with a constant ‘volatilization
29 exchange coefficient’, rather than a system of dynamically changing resistances. Rachhpal and
30 Nye (1986) made an attempt to simulate NH₃ emission from applied urea. Although this model
31 employed a constant ‘transfer coefficient’ for NH₃ volatilization as well as a constant rate of
32 urea hydrolysis were applied, the study gives an alternative for modelling the chemistry of a

Formatted: Font: 11.5 pt, German (Germany)

Formatted: German (Germany)

Formatted: Font: 8 pt, German (Germany)

Formatted: Font: 11.5 pt, German (Germany)

Formatted: Font: 11.5 pt, German (Germany)

1 urine patch, as well as the vertical distribution of the different nitrogen compounds under the
2 urine patch.

3 The present paper reports our work to construct and test a process-based, weather-driven model
4 for NH₃ emission from a urine patch, which can be applied on both field and regional scales.

5 On field scale our approach is to apply the model for every urine patch deposited over the
6 modelling period (involving statistical consideration), whilst for regional scale we are currently
7 working to incorporate the field scale model into the EMEP4UK atmospheric chemistry
8 transport model (Vieno et al., 2010, 2014). As such, the development represents a contribution
9 toward developing a comprehensive suite of weather-dependent ammonia exchange models, as
10 a necessary basis for assessing the effects of climate change on ammonia emissions and
11 deposition (Sutton et al., 2013). As soil measurements are not widely available, — especially for
12 a high resolution grid that would be required for regional scale application —, we had to account
13 for the relevant processes in the soil, such as the change of concentration of the different reduced
14 nitrogen compounds, pH and water content. On the other hand, bearing in mind our final goal
15 - a detailed investigation of weather dependency of NH₃ emission from grazing - we focused
16 predominantly on the parametrisation of the effect of meteorological variables, keeping the
17 simulation of physical and chemical soil processes as simple as possible.

18 As our future aim is to apply the model to regional scale, simplicity to enhance scalability is a key
19 aspect of the model development. For example, from a theoretical perspective, it could be attractive
20 to explicitly model the 3-dimensional dispersion of ammonia between urine patches and adjacent
21 vegetation within the canopy. However, this would be a much more complex task, which would
22 also require major simplification when developing an upscaled regional application.

23 In this paper we firstly provide the description of our model of Generation of Ammonia from
24 Grazing (GAG). Then we present the results from the ~~model validation~~ test simulation based on
25 the measurements by Laubach et al. (2012). Finally, we report the results of a sensitivity
26 analysis in relation to the uncertain model parameters as well as several meteorological
27 variables.

28

29 **2 Description of the GAG model**

30 To simulate NH₃ emission over a urine patch the GAG model calculates the TAN budget and
31 the water budget, as well as the soil pH (hydrogen ion, H⁺, budget) under the patch. For this

1 purpose, firstly, we assume that, during urination and rain events, the incoming liquid infiltrates
2 the soil to fill soil pores until the wetted soil layer reaches its field capacity. After this point we
3 neglect any further downward or upward motion (capillary rise) in the soil. On Fig. 1 this depth
4 in the soil is the bottom of the layer referred to as “urine affected layer”.

5 We also make the assumption that soil NH₃ emission occurs only from the ‘source layer’, the
6 very top layer of the wetted soil column (similarly to Riedo et al., 2002, 2002, who also assumed
7 a source layer on the top of their multilayer system), while reduced nitrogen (here the sum of
8 NH_x and urea) that infiltrates beneath this layer is assumed to be nitrified- “and no longer
9 available to NH₃ emission. This assumption allows us to handle the numerous soil pores in the
10 source layer as a single big pore – referred hereafter as ‘model soil pore’ -, the liquid content
11 of which represents the soil pores filled by liquid, while its gaseous section represents the air-
12 filled soil pores in the source layer (Fig. 1). ~~If more-~~ We assume that all the liquid (urine or rain
13 water) gets into the soil than content is at the bottom of the model soil pore can hold (more than
14 the water content of the-/ source layer at field capacity), the excess infiltrates to the deeper soil
15 layers.-

16 The input to the TAN budget is generated by hydrolysis of the urea contained within incoming
17 urine, while NH₃ emission acts as a loss from the TAN budget. Soil pH is also regulated by
18 urea hydrolysis, which is a proton (H⁺) consuming process, and by NH₃ emission which is a
19 proton producing process. The water budget is increased by rain water and the liquid content of
20 urine, whilst it is decreased by soil evaporation. ~~The model was coded in R-~~ We assume that
21 water evaporates from the “evaporation layer” (as defined by Allen et al. (1998), see in more
22 details in Section 2.5), and the soil dries from the top, that is, during evaporation a dry front
23 moves downwards in the soil. The model was coded in R, version 3.1.2 (2014-10-31) (R Core
24 Team, 2012) and the steps of the calculation are shown in Fig. 2.

Formatted: Font: 11.5 pt, German (Germany)

25 **2.1 Simulation of ammonia exchange flux**

26 As urine deposition by grazing animals typically happens on vegetated surfaces of grassland
27 we need to take into account the effect of vegetation on the total net NH₃ flux (F_t, calculating
28 as emission minus deposition) over a urine patch. Therefore, an ideal model should capture not
29 just the ground flux at the soil surface (F_g) (referred hereafter as ‘soil emission’), but also the
30 exchange with foliage (F_f), including NH₃ deposition to water and waxes on the leaf surface
31 (F_w) and the NH₃ exchange with stomata (F_{sto}).

1 To achieve this, we extended the framework of the two-layer canopy compensation point model
 2 (abbreviated in this paper to 2LCCPM) of Nemitz et al. (2001) (Fig. 3). The original exchange
 3 model calculates F_g assuming a bulk soil compensation point on the soil surface. Instead of
 4 calculating this compensation point, we derive the compensation point for our model soil pore
 5 (χ_p). To capture the constraint due to soil particles on NH_3 exchange with the soil, we added a
 6 soil resistance (R_{soil}) to the original framework.

7 Based on the analogy of electrical circuit, seven equations (Eq. (1)-(7)) can be derived to
 8 determine the five unknown fluxes (F_t , F_g , F_f , F_w , F_{sto}) and the two unknown compensation
 9 points (over the vegetation, χ_c , and over the whole canopy, χ_{z0}). Parametrising the resistances -
 10 aerodynamic (R_a) and quasi-laminar resistance (R_b) over the canopy, aerodynamic resistance
 11 within the canopy (R_{ac}), quasi-laminar resistance (R_{bg}) at the ground, soil resistance, resistance
 12 to water and wax on the leaf surface (R_w) and stomatal resistance (R_{sto}) - as well as calculating
 13 the compensation point in the soil pore and in the stomata (χ_{sto}), we get a solvable linear system
 14 of equations.

$$F_t = F_g + F_f \quad (1)$$

$$F_f = F_w + F_{\text{sto}} \quad (2)$$

$$F_t = \frac{\chi_{z0} - \chi_a}{R_a} \quad (3)$$

$$F_g = \frac{\chi_p - \chi_{z0}}{R_{ac} + R_{bg} + R_{\text{soil}}} \quad (4)$$

$$F_f = \frac{\chi_c - \chi_{z0}}{R_b} \quad (5)$$

$$\frac{F_w}{R_w} = \frac{-\chi_c}{R_w} \quad F_w = \frac{-\chi_c}{R_w} \quad (6)$$

$$\frac{F_{\text{sto}}}{R_{\text{sto}}} = \frac{\chi_{\text{sto}} - \chi_c}{R_{\text{sto}}} \quad F_{\text{sto}} = \frac{\chi_{\text{sto}} - \chi_c}{R_{\text{sto}}} \quad (7)$$

15 Assuming ~~steady state in every~~ that the changes are close to linear within a time step (~~1 hour~~ 1h),
 16 and taking the air concentration of ammonia high above the canopy (χ_a) from measurements,
 17 the system of equations was solved for every time step by using the solve function of R
 18 programming language.

2.2 Parametrisation of the resistances and stomatal compensation point (R_a , R_b , R_{ac} , R_{bg} , R_w , R_{sto} , χ_{sto})

The detailed parametrisation of the resistances and the stomatal compensation point can be found in Section S1 in the supplementary material together with all the model constants (Table S1). Here we focus on the modifications and model assumptions we made for applying the 2LCCPM of Nemitz et al. (2001) in the GAG model.

Atmospheric resistances (R_a , R_b , R_{ac} , R_{bg}) are usually derived for homogenous (virtually infinite) surfaces, which is in apparent contradiction with the current application for a single, finite urine patch. In ongoing and future work we will apply the GAG model to field and regional scales, where the meteorological measurements and the canopy specific parameters, required to calculate these resistances, can be obtained for overall canopy types. To apply atmospheric resistances to urine patches, we assume that all the required variables and parameters to calculate them are representative for the whole experimental site including every single urine patch on the field (we also compared the results from GAG with measurements from a field experiment, as detailed in Section 4).

In the original description of the 2LCCPM, Nemitz et al. gave a parametrisation for R_a as a function of u^* (friction velocity) and L (Monin-Obukhov length), which were measured in the original modelling study. In the absence of measurements to obtain u^* and L , parametrisation should be used (Eq. (S7) and Eq. (S8), respectively). As these two parameters depend on each other, we applied iteration to calculate both. For R_b we applied the formula suggested by Nemitz et al., expressed by Eq. (S12).

Following Nemitz et al., R_{ac} was assumed to be inversely proportional to u^* ($R_{ac} = \alpha u^{*-1}$). Massad et al. (2010b) recommended values for parameter α for many surface types - including grass - as well as for all of the four seasons (Table S1). Nemitz et al. applied a parametrisation for R_{bg} (sm^{-1}) for oilseed rape (Eq. (S13)). As the approach for calculation of this resistance for grasslands is not widely discussed in the literature, we adapted the one for oilseed rape for grassland. In our model, soil emission is dependent also on R_{soil} , which is larger at least by one order of magnitude than any of the atmospheric resistances. Thus, our model is not highly sensitive to this approximation for R_{bg} (for detailed analysis of the model sensitivity see Section 5).

~~The cuticular resistance (R_w) describes the effect of the water film, forming on the waxy leaf surface, on the NH_3 absorption. Exchange of ammonia is strongly linked to the presence of a~~

1 water film on the waxy leaf surface (Flechard et al., 1999). This can form even below the
 2 saturation point for pure water vapour, as a result of condensation facilitated by hygroscopic
 3 particles on the plant surface (Burkhardt et al., 1999). Therefore, the cuticular resistance (R_w)
 4 describes the effect of this water film on NH_3 absorption. The extent to which such a thin water
 5 layer is present affects the value of R_w ; however, NH_3 absorption is also dependent on the air
 6 concentration of the acidic components (especially SO_2). These compounds, decreasing the pH
 7 of the water film, favour NH_3 deposition (Flechard et al., 1999). The process is referred to as
 8 co-deposition of the different components.

9 The modelling of this phenomenon requires the knowledge of the chemical composition of the
 10 atmosphere and substantially increases model complexity. For a simpler approach, R_w (s m^{-1} ,
 11 Eq. (8)) can be estimated as a function of relative humidity (RH, %). For this purpose – similarly
 12 also to Nemitz et al. (2001) - we used the formula from Massad et al. (2010b) (based on Sutton
 13 and Fowler (1993)) with the recommended parameters in the same study ($R_{w(\text{min})}$, minimal
 14 cuticular resistance and a for grassland as reported by Horváth et al. (2005)):

$$\cancel{R_w = R_{w(\text{min})} \times \exp(a(100 - RH))} R_w = R_{w(\text{min})} \times \exp(a(100 - RH)) \quad (8)$$

15 In the original description of the 2LCCPM R_{sto} is parametrised based on Hicks et al. (1987).
 16 Instead of this, we used a more state-of-the-art approach. As in Massad et al. (2010b), the value
 17 of R_{sto} (s m^{-1} , Eq. (9)) was derived from the stomatal resistance to ozone ($R_{\text{sto}}(\text{O}_3)$, s m^{-1}), taking
 18 into account the difference between the diffusivity of the two gases ($D_{\text{O}_3} / D_{\text{NH}_3} = 1 / 1.6$). On
 19 the other hand, we parametrised $R_{\text{sto}}(\text{O}_3)$ (Eq. (10), where 41000 is the conversion from mmol
 20 $\text{O}_3 \text{ m}^{-2}$ to m s^{-1}) based on LAI (values are recommended by Massad et al. (2010b) for grass if
 21 not measured) applying the stomatal conductance (g_s , $\text{mmol O}_3 \text{ m}^{-2}$) model of Emberson et al.
 22 (2000).

$$R_{\text{sto}} = R_{\text{sto}}(\text{O}_3) \times \frac{D_{\text{O}_3}}{D_{\text{NH}_3}} \quad (9)$$

$$R_{\text{sto}}(\text{O}_3) = \left(\frac{g_s \times \text{LAI}}{41000} \right)^{-1} \quad (10)$$

23 Stomatal conductance, defined by Eq. (11), is influenced by Eq. (11) is defined based on the
 24 relative conductances that express how the openness of the stomata changes in the function of
 25 the phenological state of the plant (g_{pot}) (assuming that grass could grow equally over the year,
 26 $g_{\text{pot}} = 1$), light (g_{light}), temperature (g_{temp}), vapour pressure deficit (g_{VPD}) and soil water

1 potential (g_{SWP}). The combined effect of these, through the openness of stomata, controls g_s
 2 between its maximal value (g_{max}) and its minimal value ($g_{max} \times g_{min}$):

$$\begin{aligned} g_s &= g_{max} g_{pot} \max\{g_{min}, (g_{light} g_{temp} g_{VPD} g_{SWP})\} \\ g_s &= g_{max} g_{pot} \max\{g_{min}, (g_{light} g_{temp} g_{VPD} g_{SWP})\} \end{aligned} \quad (11)$$

3 We followed the suggested parametrisation by Emberson et al. for g_{light} , g_{temp} and g_{VPD} (see in
 4 Section S1), but applied a different approach for g_{SWP} (Eq. (12)). As the GAG model simulates
 5 the volumetric water content of the soil (θ , $m^3 m^{-3}$; see the formulation in Section 2.5) for
 6 estimating g_{SWP} - instead of using the original parametrisation depending on the soil water
 7 potential - we adapted the approach by Simpson et al. (2012), who defined a soil moisture index
 8 (S_{MI} , Eq. (13)), based on θ , influenced also by the soil's permanent wilting point (θ_{pwp}) and field
 9 capacity (θ_{fc}).

$$g_{SWP} = \begin{cases} 1 & \text{if } S_{MI} \geq 0.5 \\ 2 \times S_{MI} & \text{if } S_{MI} < 0.5 \end{cases} \quad (12)$$

$$S_{MI} = \frac{\theta - \theta_{pwp}}{\theta_{fc} - \theta_{pwp}} \quad S_{MI} = \frac{\theta - \theta_{pwp}}{\theta_{fc} - \theta_{pwp}} \quad (13)$$

10 The stomatal compensation point, as the equilibrium gaseous NH_3 concentration in the stomata,
 11 can be derived from the temperature dependent form of Henry's law for dissolution of NH_3 (R1
 12 in Table S21) and the dissociation coefficient of NH_4^+ (R4 in Table S21). Nemitz et al. (2000)
 13 derived χ_{sto} (Eq. (14)) as a function of temperature (K) and the emission potential of the stomata
 14 (Γ_{sto}), which equals to the ratio of the NH_4^+ and H^+ concentrations ($mol dm^{-3}$) in the apoplastic
 15 fluid in the stomatal cavity.

$$\chi_{sto} = \frac{161500}{T} \times \exp\left(\frac{-10380}{T}\right) \times \Gamma_{sto} \quad (14)$$

16 In the original 2LCCPM Γ_{sto} is an input parameter from measurements. Since the measurement
 17 of Γ_{sto} is very difficult, in models it is usually handled as a constant, parametrised or simulated
 18 by a sub-model (e.g. Massad et al., 2010a, Wu et al., 2009). As there were no Γ measurements
 19 in the experiment we used in the test simulation (nor would such measurements be available
 20 for regional scale application) and over a urine patch NH_3 exchange is dominated by soil
 21 emission, we chose the parametrisation recommended by Massad et al. (2010b) for grazed
 22 fields. Eq. (15) assumes that Γ_{sto} reaches its maximum $\Gamma_{sto(max)}$ right after N application (in

1 this case after urine deposition), and then decays exponentially with time (t_i indicates the time
2 step, the hours spent after urine deposition, with a decay parameter τ set at 2.88×24 hours).

$$\Gamma_{sto}(t_i) = \Gamma_{sto}(\max) \times \exp\left(-\frac{t_i - 1}{\tau}\right) \quad (15)$$

3 ~~$\Gamma_{sto}(\max)$ (Eq. (16)), from Massad et al., (2010b, is determined by) proposed a parametrization,~~
4 ~~describing an empirical relationship (Eq. (16)) between the amount of nitrogen-total N applied~~
5 ~~to the ecosystem (N_{app} ; in kg N ha^{-1} , see Eq. (17)), which in our case is the nitrogen (17)) and~~
6 ~~the observed maximal stomatal NH_3 emission potential ($\Gamma_{sto}(\max)$). To apply the formula for a~~
7 ~~urine patch, we calculated N_{app} as the total N content of the urine calculated as the volume of~~
8 ~~urine (W_{urine} , dm^3) multiplied by its nitrogen content (c_N , $\text{g N g N}^{-1} \text{dm}^{-3}$), - divided by the area~~
9 ~~of the urine patch (A_{patch} , m^2) (with 10 as a conversion factor between the different units).~~

$$\Gamma_{sto}(\max) = 12.3 \times N_{app} + 20.3 \quad (16)$$

10

$$N_{app} = \frac{W_{urine} \times c_N}{A_{patch}} \times 10 \quad (17)$$

Formatted: Not Superscript/ Subscript

11 2.3 Simulation of the soil pore (χ_p) compensation point and the soil resistance 12 (R_{soil})

13 The simulation of χ_p (mol dm^{-3}) is very similar in theory to that of χ_{sto} , being derived from
14 Henry's law for NH_3 dissolution and the dissociation coefficient of NH_4^+ . In this way we get
15 Eq. (18) (Nemitz et al., 2000), where T_{soil} is the soil temperature (K) and Γ_p is the ratio of the
16 NH_4^+ and H^+ concentration in the model soil pore. In Eq. (19) Γ_p is expressed as a function of
17 TAN concentration ($[\text{TAN}] = [\text{NH}_4^+] + [\text{NH}_3(\text{aq})]$) based on the definition of dissociation
18 constant ($K(\text{NH}_4^+)$, second column of Table S21 and its temperature dependent form in the third
19 column).

$$\chi_p = \frac{161500}{T_{soil}} \times \exp\left(\frac{-10380}{T_{soil}}\right) \times \Gamma_p \quad (18)$$

$$\Gamma_p = \frac{[\text{TAN}]}{K(\text{NH}_4^+) + [\text{H}^+]} \quad (19)$$

1 TAN and H⁺ concentration (both in mol dm⁻³) are derived from TAN budget (B_{TAN}, g N) and
 2 H⁺ budget (B_{H⁺}, mol), according to their mass ratio with water budget (B_{H₂O}, dm³) (Eqs. (20)-
 3 (21)), where 14 is the molar mass of nitrogen). All budgets are simulated within GAG (see
 4 B_{TAN}: Section 2.4, B_{H⁺}: Section 2.6, and B_{H₂O}: Section 2.5).

$$[TAN] = \frac{B_{TAN}}{B_{H_2O}} \cdot \frac{14}{1} \quad (20)$$

$$[H^+] = \frac{B_{H^+}}{B_{H_2O}} \quad (21)$$

5 For R_{soil} (s m⁻¹) we applied the approach by Laubach et al. (2012), as expressed in Eq. (22).
 6 This captures the effect of soil depth (Δz), that is, from how deep the soil NH₃ emission occurs
 7 on average. In the study of Laubach et al. Δz is referred as ‘source depth’, and in GAG model
 8 we consider it as the thickness of the source layer. The ~~inverse~~ model experiments by Laubach
 9 et al. suggested that the distribution of Δz has a median of 0.002 m with an uncertainty factor
 10 of 2 and a similar value (0.003 m) was used in the study of Riedo et al. (2002) as well. In reality
 11 the thickness of the source layer changes parallel with the moisture content of the top soil layer;
 12 however, its approximation, due to the thinness of the layer, is difficult. Therefore, at the
 13 moment our model operates with a constant Δz of 0.004 m. (In Section 5.2 we tested the model
 14 sensitivity also to Δz.)

$$R_{soil} = \frac{\Delta z}{\xi D_g} \quad (22)$$

15 According to this approach, R_{soil} is inversely proportional to soil tortuosity (ξ) and diffusivity
 16 of NH₃ (D_g). For ξ, Laubach et al. (2012) suggested the parametrisation by Millington and
 17 Quirk (1961), based on the volumetric water content as well as porosity (θ_{por}):

$$\xi = \frac{(\theta_{por} - \theta)^{10}}{\theta_{por}^2} \quad (23)$$

Formatted: Font: Not Bold, Not Raised by / Lowered by

Formatted: Font: Not Bold

Formatted Table

Formatted: Centered

18 2.4 Simulation of the TAN budget under the urine patch (B_{TAN})

19 The amount of TAN in the model soil pore in a given time step t_i (B_{TAN}(t_i), g N), depends on
 20 its value in the previous time step (B_{TAN}(t_{i-1}), g N) and is controlled by the amount of TAN
 21 produced during urea hydrolysis (N_{prod}, g N) and soil NH₃ emission (F_g, g N m⁻²) calculated in

1 the previous time step (Eq. (24)). We assume that B_{TAN} before urine deposition is
 2 negligibly small (compared to that of after urine deposition). Therefore, its initial
 3 value is set to 0. In the first time step (right after depositing urine), as well as if all the
 4 The model does not allow to emit more NH_3 than TAN was emitted as NH_3 is available in the previous time
 5 step, B_{TAN} equals to N_{prod} source layer, as it is described by Eq. 25.

$$B_{TAN}(t_i) = \begin{cases} N_{prod}(t_i) & \text{if } (B_{TAN}(t_{i-1}) - F_g(t_{i-1}) \times A_{patch}) < 0 \\ N_{prod}(t_i) + B_{TAN}(t_{i-1}) - F_g(t_{i-1}) \times A_{patch} & \text{otherwise} \end{cases} \quad (24)$$

$$F_g = \begin{cases} \frac{B_{TAN}(t_{i-1})}{A_{patch}} & \text{if } (B_{TAN}(t_{i-1}) - F_g(t_{i-1}) \times A_{patch}) < 0 \\ \frac{\chi_p - \chi_{z_0}}{R_{ac} + R_{bg} + R_{soil}} & \text{otherwise} \end{cases} \quad (25)$$

6 TAN production depends on the current amount of urea nitrogen within the model soil pore
 7 (B_{urea} , g N), as well as soil temperature (T_{soil} , °C). For N_{prod} Sherlock and Goh (1985) suggested
 8 an empirical formula (Eq.(26)), with a temperature dependent parameter (A_h , Eq. (27)) and a
 9 hydrolysis constant (k_h , see Table 4).

$$N_{prod}(t_i) = B_{urea}(t_i) (1 - \exp(-A_h(t_i) \times k_h)) \quad (26)$$

$$A_h(t_i) = 0.25 \times \exp(0.0693 \times T(t_i)) \quad A_h(t_i) = 0.25 \times \exp(0.0693 \times T_{soil}(t_i)) \quad (27)$$

10 Urea nitrogen content in a given time step (Eq. (28)) is determined by its value in the previous
 11 time step, the loss as conversion to TAN ($-N_{prod}$) and, in the first time step, the amount of urea
 12 nitrogen added (U_{add} , g N) with the incoming urine. In U_{add} (Eq.(29)) we take into account the
 13 dilution effect of rain and soil water on the nitrogen concentration of urine (c_n). We assume,
 14 that right after urine deposition the urea nitrogen content of urine, diluting in the total soil water
 15 ($B_{H_2O}^{Tot}$, Eq. (31)), forms a homogenous soil solution with a concentration of c_n^{Tot} (Eq. (30)).
 16 Finally, U_{add} is calculated as the product of c_n^{Tot} and the water content of the emission layer.
 17 (This will equal to $B_{H_2O}^{Tot}$ unless there is more water in the soil than can be stored in the
 18 emission layer, as indicated by $B_{H_2O}(max)$, which is specified in the following section, see Eq.
 19 (35)).

$$B_{urea}(t_i) = B_{urea}(t_{i-1}) - N_{prod}(t_{i-1}) + U_{add}(t_i) \quad (28)$$

Formatted: Font: 11.5 pt, German (Germany)

Formatted: Font: 11.5 pt, German (Germany)

Formatted: Font: 11.5 pt, German (Germany)

$$U_{add} = c_n^{Tot} \min\{B_{H_2O}(\max), B_{H_2O}^{Tot}\} \quad (29)$$

$$c_n^{Tot} = c_n \frac{W_{urine}}{B_{H_2O}^{Tot}} \quad (30)$$

1 2.5 Simulation of the water budget under the urine patch ($B_{H_2O}^{Tot}$, θ , B_{H_2O} , 2 $B_{H_2O}(\max)$)

3 The soil moisture content affects NH_3 emission in several ways. In the first time step when the
4 urine is deposited, both the water content of the model soil pore and the water content of the
5 whole urine-affected soil layer ($B_{H_2O}^{Tot}$, Eq. (31)) have an effect on emission. The thickness of
6 the urine-affected soil layer depends on the amount of incoming liquids: urine (considering its
7 whole volume as water) and rain (W_{rain} , dm^3). The more water is added, the more empty soil
8 pore it can fill up and consequently, the deeper it will infiltrate.

9 We made the assumption for our model that the lowest possible volumetric water content in the
10 soil is at permanent wilting point (θ_{pwp}) and the highest is at the field capacity (θ_{fc}), where both
11 θ_{pwp} and θ_{fc} are expressed as fractions of total soil volume. Assuming that the initial soil water
12 content is at θ_{pwp} , and after infiltration it rises to θ_{fc} , the volume fraction taken up by the
13 incoming water will be $\theta_{fc} - \theta_{pwp}$. Finally, we get the total water content (incoming + soil water)
14 in the urine-affected layer (having a volumetric water content of θ_{fc}) as:

$$B_{H_2O}^{Tot} = (W_{rain}(t_1) + W_{urine}) \frac{\theta_{fc}}{\theta_{fc} - \theta_{pwp}} \quad (31)$$

15 After urine deposition, actual volumetric water content (θ , Eq. (32)) of the source layer can be
16 expressed as the volume of the water in the layer (B_{H_2O} , dm^3) divided by the volume of the soil
17 column under the urine patch with a surface area of A_{patch} (m^2) and a thickness of Δz (m) (in
18 Eq. (31), 1000 is the conversion from m^3 to dm^3).

$$\theta = \frac{B_{H_2O}}{1000 \times \Delta z \times A_{patch}} \quad (32)$$

19 The actual water content of the soil at any time step ($B_{H_2O}(t_i)$, Eq. (33)) depends on the water
20 content in the previous time step, soil evaporation (W_{evap} , dm^3), rain events (W_{rain} , dm^3) and in
21 the very first time step the volume of urine (e.g. if the volume of the urine is $1.5 dm^3$ then
22 $W_{urine}(t_1) = 1.5 dm^3$, otherwise 0). Both the volume of evaporation from the source layer and

1 incoming rain to this layer are derived as the product of A_{patch} and soil evaporation (with E (dm^3
2 m^{-2}): $W_{\text{evap}} = E \times A_{\text{patch}}$) as well as precipitation (with P ($\text{dm}^3 \text{m}^{-2}$): $W_{\text{rain}} = P \times A_{\text{patch}}$) for a m^2 ,
3 respectively.

$$B_{H_2O}'(t_i) = \begin{cases} B_{H_2O}(\min) + W_{\text{rain}}(t_i) + W_{\text{urine}}(t_i) & \text{if } (B_{H_2O}(t_{i-1}) - W_{\text{evap}}(t_{i-1})) < B_{H_2O}(\min) \\ B_{H_2O}(t_{i-1}) - W_{\text{evap}}(t_{i-1}) + W_{\text{rain}}(t_i) + W_{\text{urine}}(t_i) & \text{otherwise} \end{cases} \quad (33)$$

4 It is not possible for more water to be evaporated from the source layer than the minimal water
5 content (water content of the layer at θ_{pwp} : $B_{H_2O}(\min)$ (dm^3), Eq. (34)). On the other hand, (as
6 is shown in Eq. (35)) this layer cannot store more water than the maximal water content (water
7 content of the layer at θ_{fc} : $B_{H_2O}(\max)$ (dm^3), Eq. (36)). The excess water is assumed to infiltrate
8 to the deeper soil layers. (In Eq. (34) and (36) 1000 is the conversion from m^3 to dm^3 .)

$$B_{H_2O}(\min) = 1000 \times \Delta z \times A_{\text{patch}} \times \theta_{\text{pwp}} \quad (34)$$

$$B_{H_2O}(t_i) = \min\{B_{H_2O}'(t_i), B_{H_2O}(\max)\} \quad (35)$$

$$B_{H_2O}(\max) = 1000 \times \Delta z \times A_{\text{patch}} \times \theta_{\text{fc}} \quad (36)$$

9 Instead of constructing a comprehensive energy balance model for GAG (driving NH_3 and
10 water vapour flux in the same time), -for simplicity's sake, to estimate the soil evaporation we
11 adapted the dual crop method of Allen et al. (1998). The approach firstly calculates the
12 reference evapotranspiration (ET_0 , evaporation from soil + transpiration by plants) for a
13 reference surface (a surface covered by grass with a height of 0.12 m, a fixed surface resistance
14 to water exchange of 70 s m^{-1} and albedo of 0.23). Then, defining a 'crop coefficient' (K_c) for
15 the actual surface, it gives an estimation for the actual evapotranspiration ($ET = K_c \times ET_0$). In
16 the final step K_c is split to a coefficient for transpiration and a coefficient for soil evaporation
17 ($K_c = K_{\text{cb}} + K_e$).

18 In our model for ET_0 we incorporated a slightly modified form of the Penman-Monteith
19 equation (Eq.(37), Walter et al., 2001) compared with that of Allen et al. (1998). In this way
20 the model accounts for the effect of change of day and night on evapotranspiration (C_d , Eq.
21 (38)). For the formulation of Δ (the slope of the saturation vapour pressure temperature
22 relationship), R_n (net radiation), G (soil heat flux) and γ (psychrometric constant), see the details
23 in Allen et al. (1998).

$$ET_0 = \frac{0.408 \times \Delta(R_n - G) + \gamma \frac{37}{T + 273.15} u(e_s - e_a)}{\Delta + \gamma(1 + C_d u)} \quad (37)$$

$$C_d = \begin{cases} 0.24 & \text{if } R_n > 0 \quad (\text{daytime}) \\ 0.96 & \text{otherwise} \quad (\text{nighttime}) \end{cases} \quad (38)$$

1 When calculating soil evaporation ($E = K_e \times ET_0$) we made the following assumptions:

- 2 - According to Allen et al. soil evaporation occurs from the wetted, uncovered soil
3 fraction (f_w). Applying the evapotranspiration model for a urine patch, the whole
4 modelled soil will be wet. In addition, we assumed that the percentage of the whole field
5 covered by vegetation (f_c) is the same over a urine patch. In this way $f_w = (1 - f_c)$ for a
6 urine patch.
- 7 - Following the recommendations of Allen et al., we assumed that there is no runoff, no
8 transpiration from the evaporation layer (including the NH_3 source layer) and no ‘deep
9 percolation’ (which occurs when θ exceeds θ_{fc} , but in our model θ_{fc} is assumed to be the
10 maximum of θ).
- 11 - In the original approach it is assumed that soil evaporation attenuates when more water
12 is evaporated from the soil evaporation layer (characterized by a thickness of Δz_E) than
13 the amount of ‘readily evaporable water’ (REW). The study of Allen et al. recommends
14 REW values for different soil types defined by their θ_{fc} and θ_{pwp} . However, for the
15 ~~validation site of whose measurement we used in the present study~~ test simulation (see
16 Section 4.2.1), with a sandy loam soil, these θ_{fc} and θ_{pwp} values were not in accordance
17 with the measurements. Therefore, we calculated REW as the water content of the
18 evaporation layer halfway between θ_{fc} and θ_{pwp} :

$$REW = 1000(\theta_{fc} - 0.5(\theta_{fc} - \theta_{pwp})) \times \Delta z_E \quad (39)$$

19 The model constants used in the soil evaporation estimation are listed in Table [S3S2](#).

20 2.6 Simulation of soil pH (B_{H^+})

21 After urine deposition, soil pH is affected by two main reactions: urea hydrolysis and NH_3
22 emission. When a urea molecule is decomposed (based on R0 in Table 1) an H^+ ion is
23 consumed, producing two NH_4^+ ions and a bicarbonate ion (HCO_3^-). In the early stages of urea
24 hydrolysis, when a large amount of urea is hydrolysed, a large amount of H^+ is required,

1 resulting in a peak of soil pH (minimum of soil H^+ concentration). This triggers the dissociation
2 of the produced NH_4^+ and consequently the formation of gaseous ammonia, which also leads
3 to an emission peak shortly after urine deposition. Once the majority of urea has been
4 hydrolysed, ammonia emission may still be continuing. To balance the lost gaseous ammonia,
5 more NH_4^+ dissociates, resulting in H^+ production, which tends to compensate the H^+
6 consumption associated with urea hydrolysis.

7 According to Sherlock and Goh, (1985) after a rapid increase, soil pH usually peaks around 6-
8 48 hours after urine deposition (referred to as 'first stage' of emission). Subsequently, the pH
9 tends to drop for the reasons explained above over a period of about 2-8 days (second stage).
10 Sherlock and Goh also identified two further stages: a 1-3 week long constant phase (third
11 stage) when soil pH does not change considerably and, finally, a phase (fourth stage) with a
12 moderate decline in soil pH, regulated by the nitrification of TAN.

13 As Sherlock and Goh (1985) pointed out that the bulk of TAN is volatilized over the first and
14 second periods, and nitrification is a sufficiently slower process than NH_3 volatilization (see
15 the cited references in the study of Sherlock and Goh), in the GAG model we neglect the effect
16 of nitrification. On the other hand, we make the assumption that the solid material of soil is
17 chemically inert, and consequently, NH_3 emission from soil is only affected by the composition
18 of urine solution. ~~To~~

19 Whitehead et al. (1989) showed that not only urea but other urinary nitrogen components, such
20 as allantoin, creatine and creatinine, can contribute to NH_3 emission through their
21 decomposition. However, Whitehead et al. found that only allantoin can have a comparable
22 influence on NH_3 volatilization (from the solutions of these compounds with the same N
23 concentration, over 8 days 15% of the applied N was emitted from urea and 11% from the
24 allantoin); that of the other two components, creatine and creatinine, is rather small (over 8 days
25 4% and less than 1% of the applied N was emitted as NH_3 , respectively). In addition, according
26 to Dijkstra et al. (2013) the proportion of allantoin in urinary nitrogen is considerably lower
27 than that of urea, 2.2-14.2% compared to 57.8-93.5% and the proportions for creatine and
28 creatinine are even lower. Therefore, to further focus our model onto the key reactions, we
29 simulate urine chemistry considering only the water and urea available in the beginning, and
30 the products of urea breakdown afterwards.

31 As urine is a relatively concentrated solution, non-ideal ionic behaviour may have an effect on
32 the chemical equilibria. To test this in the model, we did a test run with the maximum activity

1 coefficients derived for the highest ion concentrations (0.2 mol dm⁻³) published by Kielland
2 (1937) (the highest ionic concentration in the modelled solution was 0.14 mol dm⁻³). With this
3 modification, the difference, in the total NH₃ emission was -4.7% and the average change in
4 pH was -0.019. Considering, that the ion concentration decreases toward the end of the
5 modelling period, and consequently, the activity coefficients converge to 1, we neglect the
6 effect of non-ideal behaviour in the solution.

7 In this way, we consider the reactions for change of soil pH listed in Table S21: urea hydrolysis
8 (R0), NH₄⁺ dissociation (R1), dissociation of HCO₃⁻ and H₂CO₃ (carbonic acid) (R2 and R3,
9 respectively), formation of gaseous NH₃ and CO₂ (carbon dioxide) (R4 and R5, respectively).
10 However, considering that soil is a buffered system, we also incorporate a soil buffering
11 capacity (β mol H⁺ (pH unit)⁻¹ dm⁻³). Buffering capacity moderates the change of H⁺ ion
12 concentration. When H⁺ ions are produced in the system during urea hydrolysis and the related
13 equilibrium processes, to balance this change H⁺ ions are consumed by buffers, and similarly,
14 when H⁺ ions are consumed in the system, buffers releases H⁺ ions. In the model this buffering
15 effect is expressed by the term of $\beta_{\text{patch}}(\text{pH}(t_i) - \text{pH}(t_{i-1}))$ in Eq. 46. This term is positive when the
16 H⁺ ion concentration decreases (pH increases), and it is negative in the opposite case.

17 Whitehead and Raistrick (1993) found a strong correlation between the cation exchange
18 capacity (CEC) and NH₃ volatilization as well as a weaker correlation with organic matter, clay
19 and sand content of the soil. However, we are not aware of a specific quantitative relationship
20 between buffering capacity and CEC, or the clay content or the organic matter content.
21 Therefore, we address this issue through a sensitivity analysis on the model performance
22 (Section 5.3).

23 Regarding the effect of the potassium content of urine on buffering capacity and indirectly, NH₃
24 emission, Whitehead et al. (1989) showed that the potassium salts of urine have a rather small
25 influence on NH₃ volatilization. Based on these, we used a constant buffering capacity in the
26 model. We defined β during test simulations with GAG. We found, that the model represents
27 the measured pH the bestwell with a β of 0.021 mol H⁺ (pH unit)⁻¹ dm⁻³. To get the buffering
28 effect in the volume of our model soil pore we calculated $\beta_{\text{patch}} = \beta \times A_{\text{patch}} \times \Delta z$. (For a
29 sensitivity analysis to β see Section Sect. 5.3.)

30 We defined 13 equations to calculate soil pH (Eqs. (40)-(52)), eight of which are predictive
31 equations, Eqs. (40)-(47), where B_X (mol) is the budget of the component X in the urine solution
32 and r_{RX} (mol) is the production or consumption of a giventhe compound predicted by the given

Formatted: Font: 11.5 pt, German (Germany)

Formatted: Font: 11.5 pt, German (Germany)

1 equation in the reaction X- (following the numbering of reactions in Table 1). Variables i_N and i_C
 2 indicate the nitrogen and carbon input generated during urea hydrolysis, respectively. The
 3 nitrogen input is the same as N_{prod} but in mol ($i_N = N_{\text{prod}} / 14$) and based on R_0 , $i_C = i_N / 2$.

4 The other five equations describe the equilibrium in every time step (Eqs. (48)-(52)). These
 5 were derived by reorganizing the equations in the second column in Table S21, where, for a
 6 dissolved component X: $[X] = B_X / B_{H_2O}$ and for a gaseous component $X_{(g)}$: $[X_{(g)}] = B_{X(g)} / V_{\text{air}}$.
 7 V_{air} is the volume of the air in the model soil pore, which can be calculated as the volume of
 8 the space in the model soil pore that is not taken up by the liquid content
 9 ($V_{\text{air}} = \theta_{\text{por}} A_{\text{patch}} \Delta Z \times 1000 - B_{H_2O}$, where 1000 is the conversion between m^3 and dm^3).

10 Variables B_C and B_N represent the total inorganic carbon and nitrogen budget in the urine
 11 solution, respectively. Both can be derived as a sum of the different components and their input
 12 (by urea breakdown) and loss (via emission as gas) (Eqs. (53) and (54)).

$$B_{H_2CO_3}(t_i) = B_{H_2CO_3}(t_{i-1}) + (-r_{R5} + r_{R3}) \quad (40)$$

$$B_{HCO_3^-}(t_i) = B_{HCO_3^-}(t_{i-1}) + (-r_{R2} - r_{R3} + i_C(t_i)) \quad (41)$$

$$B_{CO_3^{2-}}(t_i) = B_{CO_3^{2-}}(t_{i-1}) + r_{R2} \quad (42)$$

$$B_{CO_{2(g)}}(t_i) = B_{CO_{2(g)}}(t_{i-1}) + r_{R5} \quad (43)$$

$$B_{NH_4^+}(t_i) = B_{NH_4^+}(t_{i-1}) + (-r_{R1} + i_N(t_i)) \quad (44)$$

$$B_{NH_{3(aq)}}(t_i) = B_{NH_{3(aq)}}(t_{i-1}) + (r_{R1} - r_{R4}) \quad (45)$$

$$B_{NH_{3(g)}}(t_i) = B_{NH_{3(g)}}(t_{i-1}) + \left(r_{R4} - \frac{F_g(t_{i-1}) \times A_{\text{patch}}}{14} \right) \quad (46)$$

$$B_{H^+}(t_i) = B_{H^+}(t_{i-1}) - i_C(t_i) + (-r_{R3} + r_{R2} + r_{R1}) + \beta_{\text{patch}}(pH(t_i) - pH(t_{i-1})) \quad (47)$$

$$K(NH_4^+)(t_i) B_{H_2O}(t_i) B_{NH_4^+}(t_i) - B_{H^+}(t_i) B_{NH_{3(aq)}}(t_i) = 0 \quad (48)$$

$$K(CO_3^{2-})(t_i) B_{H_2O}(t_i) B_{HCO_3^-}(t_i) - B_{H^+}(t_i) B_{CO_3^{2-}}(t_i) = 0 \quad (49)$$

$$K(H_2CO_3)(t_i) B_{H_2O}(t_i) B_{H_2CO_3}(t_i) - B_{H^+}(t_i) B_{HCO_3^-}(t_i) = 0 \quad (50)$$

Formatted: Font: 11.5 pt, German (Germany)

Formatted: Font: 11.5 pt, German (Germany)

$$\begin{aligned} & \left(H(\text{CO}_{2(g)})(t_i) \frac{B_{\text{H}_2\text{O}}(t_i)}{V_{\text{air}}(t_i)} + 1 \right) B_{\text{H}_2\text{CO}_3}(t_i) + H(\text{CO}_{2(g)})(t_i) \frac{B_{\text{H}_2\text{O}}(t_i)}{V_{\text{air}}(t_i)} B_{\text{HCO}_3^-}(t_i) + H(\text{CO}_{2(g)})(t_i) \frac{B_{\text{H}_2\text{O}}(t_i)}{V_{\text{air}}(t_i)} B_{\text{CO}_2}(t_i) = \\ & = H(\text{CO}_{2(g)})(t_i) \frac{B_{\text{H}_2\text{O}}(t_i)}{V_{\text{air}}(t_i)} B_C(t_i) \end{aligned} \quad (51)$$

$$\begin{aligned} & \left(H(\text{NH}_{3(g)})(t_i) \frac{B_{\text{H}_2\text{O}}(t_i)}{V_{\text{air}}(t_i)} + 1 \right) B_{\text{NH}_3(aq)}(t_i) + H(\text{NH}_{3(g)})(t_i) \frac{B_{\text{H}_2\text{O}}(t_i)}{V_{\text{air}}(t_i)} B_{\text{NH}_4^+}(t_i) = \\ & = H(\text{NH}_{3(g)})(t_i) \frac{B_{\text{H}_2\text{O}}(t_i)}{V_{\text{air}}(t_i)} B_N(t_i) \end{aligned} \quad (52)$$

$$B_C(t_i) = B_{\text{H}_2\text{CO}_3}(t_{i-1}) + B_{\text{HCO}_3^-}(t_{i-1}) + B_{\text{CO}_3^{2-}}(t_{i-1}) + B_{\text{CO}_2}(t_{i-1}) + i_C(t_i) \quad (53)$$

$$B_N(t_i) = B_{\text{NH}_3(aq)}(t_{i-1}) + B_{\text{NH}_4^+}(t_{i-1}) + B_{\text{NH}_3(g)}(t_{i-1}) + i_N(t_i) - \frac{F_g(t_{i-1}) \times A_{\text{patch}}}{14} \quad (54)$$

1 Although references can be found in the literature for measurements of CO₂ emission from
 2 urine patches (e.g. Wang et al., 2013, Ma et al., 2006 and Lin et al., 2009), we considered that
 3 the driving processes behind them are not well-enough described for an hourly model
 4 application. Therefore, in the case of the carbon budget (Eq. 53) we ~~assumed not did not assume~~
 5 a term for CO₂ emission in the basic GAG model, but we tested the effect of CO₂ emission in
 6 Section 5.3. The dissociation coefficients (K(X)(t_i)) and Henry constants (H(X(g))(t_i)) for the
 7 given t_i time step were derived as a function of actual soil temperature (third column of Table
 8 S21).

9 For a given B_{H⁺}(t_i) Eqs. (40)-(46) and Eqs. (48)-(52) constitute a linear system of equations (12
 10 equations, and seven B_X(t_i) budgets and five r_{Rx} consumptions/productions as unknowns). As
 11 B_{H⁺}(t_i) is unknown, we are looking for a solution with a particular B_{H⁺}* for this equation system,
 12 whose roots also satisfy Eq.(47), giving back B_{H⁺}*. For this purpose, we used the uniroot
 13 function of programming language R (version 3.1.2 (2014-10-31)), which is able to look up find
 14 this B_{H⁺}*. B_{H⁺}* provides the H⁺ budget in the given time step and finally, pH can be calculated
 15 as pH = ~~-log~~ -log₁₀ (B_{H⁺}* / B_{H₂O}).

3 Validation data

Formatted: Font: Not Bold

3 Measurement data used in the test simulation

The GAG model described in the preceding sections was developed to simulate NH_3 emission from a single urine patch. However, for ~~validation~~testing the model we chose a field experiment where the NH_3 emission flux was measured from several urine patches deposited relatively close in time. The only experiment we are aware of with these features was conducted by Laubach et al. (2012), who measured the NH_3 fluxes over a field covered with a regular pattern of urine patches.

In the experiment, 156 artificial urine patches were deposited within 45 minutes (see an overview of urine patch characteristics in Table 42) over a circular plot at an experimental site, in Lincoln New Zealand. In the middle of the plot NH_3 concentration was measured at five heights with Leuning samplers (Leuning et al., 1985) from which the fluxes were derived by different methods. For this study we used the fluxes calculated by Laubach et al. according to the mass balance (MB) method.

Soil samples were taken from 24 patches on the edge of the plot to measure soil pH, volumetric water content and mineral N content. Soil temperature was measured at two heights, and meteorological measurements were also carried out (from which we used wind speed, temperature, photosynthetically active radiation (PAR), sensible heat flux and atmospheric pressure data). For more details on measurements and flux calculation, see Laubach et al. (2012).

In addition to the available measurements, we also needed meteorological data that were not measured in the experiment: global radiation (R_{glob}) and RH. We obtained these data from the National Climate Database for New Zealand (NIWA, 2015).

We ~~validated~~compared our model results ~~against~~with measurements of F_i , soil pH and θ for the measurement period between 24/02/2010 11:30 AM and 01/03/2010 1:30 AM. In the case of F_i , the length of the collecting period of each measurement varied mostly between 1-1.5 hour for daytime measurements, and 7-7.5 hours for the night-time measurements. As the time step of our model is 1 hour and emission fluxes were not expected to change considerably over the night, we assumed that the measured average NH_3 flux over the collecting period is representative for the midpoint of the period, and we compared these to our model values in the time step closest to the midpoint of the corresponding measurements.

1 In addition, assuming that the change of the soil's mineral reduced nitrogen content ($\text{NH}_x\text{-N}$) is
2 parallel with the B_{TAN} in the model soil pore, we also compared these two parameters. All of
3 the input data, as well as ~~validation data~~the measurement data we used to compare our model
4 results, together with their modification for our hourly model run, are listed in Table 23.

5 To compare the measured and modelled F_t for a single urine patch, we assumed that the great
6 majority of NH_3 in the experiment of Laubach et al. (2012) was emitted from the urine patches.
7 Therefore, we multiplied the observed fluxes by the effective source area (804.9 m^2 as
8 calculated by Laubach et al. (2012)), then divided it by the total area of the deposited 156
9 patches ($F_t^{\text{single}} = F_t \times 804.9 / (156 \times A_{\text{patch}})$). ~~To validate the simulation of θ we also ran the~~
10 ~~model with a Δz of 5 mm (instead of the original setting of 4 mm as shown in Table 1), so that~~
11 ~~it was comparable with the measurements for which soil samples were taken by using a sharp-~~
12 ~~edged metal ring that was pushed to about 5 mm to the soil.~~Eq. (55), F_t^{single} stands for the
13 converted measured flux).

14

15 **4—Model validation**

$$16 \quad F_t^{\text{single}} = F_t \times 804.9 / (156 \times A_{\text{patch}}) \quad (55)$$

16 To compare θ with the observations, we had to consider that the θ measurements were taken by
17 using a sharp-edged metal ring that was pushed to about 5mm to the soil. As the model simulates
18 the water content of a 4 mm thick layer, the same water loss via evaporation would not result
19 in the same volumetric water content as was measured in the 5 mm depth sample. Since none
20 of the other soil modules have effect on the water budget, we ran the model also with a Δz of 5
21 mm to get results that are comparable with the measurements.

22

23 **4 Test simulation**

24 The results of the ~~model validation~~test simulation are summarized in Fig. 4 and ~~Table 3.~~Table
25 4. GAG captures the emission relatively well. ~~We got a significant and~~Considering, that
26 compared to the complexity of the phenomena, we use a simple model, the Person's correlation
27 coefficient (hereafter referred to as "correlation") for NH_3 flux, can be considered as relatively
28 high ~~correlation of~~ ($r=0.54$ ~~with measurements.~~, $p=0.01$). The model slightly overestimates the
29 fluxes before the rain event on the second day and it rather underestimates the measured values
30 after it. The total emissions over the whole period from a single patch (modelled: 1.78 g N,

1 measured: 3.88 g N) was underestimated. However, the model is still capable of reproducing
2 the daily pattern of emissions with the mid-day peaks (except on the second day).

3 Soil pH is well simulated before the rain event, but similarly to the emission fluxes, it is
4 underestimated afterwards. Overall there was a high and significant correlation ($r=0.75$),
5 between the model and the measurements. The sudden pH drop at the beginning of the rain
6 event is thought to be caused by the lack of handling of CO₂ emission in the basic version of
7 the model (see Section 5.3 for further examination of this effect).

8 Despite the large error bars on the measured mineral reduced soil N, its tendency is fairly similar
9 to that of the TAN budget simulated by GAG. This is supported also by the significant
10 correlation ($r=0.63$) between the two parameters/variables. The model performance in terms of
11 volumetric water content is very good with a slight underestimation from the fourth day after
12 urine application. The statistical analysis showed a high correlation of 0.92 at a 0.001
13 significance level.

14 Analysing the NH₃ emission, pH and TAN budget together, it can be concluded that the rain
15 event affected all three parameters/variables considerably. As it can be seen in the measured
16 NH_x-N and pH dataset (Fig. 4.), their values right after the rain event peaked close to the level
17 (or even higher) of the first peaks, which were generated by urea hydrolysis. This suggests that
18 urea breakdown might restart after the rain event, explaining the difference between the
19 modelled and measured values.

20 The GAG model used here does not account for any retention of urine by vegetation; however,
21 it is possible that this occurs in reality. For example, Doak (1952) found that the urine held on
22 the leaf surfaces was 36% of fresh herbage weight. In addition, the model assumptions do not
23 allow the model soil pore to dry out (the minimum water content is at the permanent wilting
24 point). In reality, however, the moisture content of urine retained on the leaf surfaces can
25 evaporate easily and also some soil pores can completely dry out leaving behind the urine
26 components undissolved. In such dry conditions, in lack of water urea hydrolysis stops. Then,
27 after a rainfall, urea gets dissolved (as well as from the leaf surface it is washed into the soil)
28 and hydrolysis can begin again, leading to a high peak in pH, TAN budget and consequently,
29 NH₃ emission (see the further model results presented in Section S5S4).

30

1 **5 Sensitivity analysis for non-meteorological parameters**

2 In the following subsections we investigated module by module (2LCCPM, TAN budget, soil
3 pH and water budget), how the model responds if we change the most critical model features.

4 In the case of the model constants, we tested how the modelled total emitted NH_3 (1.78 g N
5 from a urine patch) changes over the modelling period by increasing and decreasing the given
6 assumed model constant by 10 and 20%. An overview of the results can be seen in Table 45.

7 Comments on this table are provided in the following ~~sections~~ subsections.

8 **5.1 Sensitivity to atmospheric resistances**

9 As the net NH_3 flux is dominated by the soil emission flux (shown in Fig. S1) we investigated
10 here only the influence of the atmospheric resistances that affect the soil emission: R_{soil} , R_{bg} ,
11 R_{ac} and R_{a} . In Fig. 5, on the logarithmic scale it can be clearly seen that R_{ac} is the only
12 atmospheric resistance that reaches the magnitude of the estimated R_{soil} .

13 For the simulation the main driver in temporal variation in R_{soil} is the actual volumetric water
14 content (see Fig. 4). In the case of R_{a} , R_{b} , and R_{bg} there is at least on order of magnitude
15 difference compared to the soil resistance, illustrating how the model performance is much less
16 sensitive to the exact values of R_{a} , R_{ac} , and R_{bg} . The close temporal correlation of all these
17 atmospheric resistances illustrates how they are all controlled by variations in wind speed and
18 stability for a single canopy type. All the atmospheric resistances are the closest to the soil
19 resistance when weak wind (large atmospheric resistances) is coupled to dry soil conditions
20 (small soil resistance).

21 Among R_{bg} , R_{ac} and R_{a} , the parametrisation of R_{bg} is the most uncertain. As Table 45 shows,
22 the model is hardly sensitive to the value of z_1 . In addition, u_{*g} , as formulated by Nemitz et al.
23 (2001), (Eq. (S15)), can also change in wide ranges without significantly affecting soil
24 emission: R_{bg} could overcome the effect of R_{soil} on NH_3 emission only with a 10 times higher
25 value of u_{*g} .

26 **5.2 Sensitivity to the estimation of the TAN budget**

27 The two uncertain factors in the estimation of the TAN budget are the thickness of the source
28 layer (Δz) and the area of the patch (A_{patch}). Originally the model was run with a Δz of 4 mm;
29 however, the sensitivity analysis showed (Table 45) that the change in total emission is

1 approximately half of the change in Δz . Therefore, this source of error must be considered when
2 model results are evaluated.

3 We also tested the model with Δz values between the ranges reported by Laubach et al. (2012)
4 (Fig. 6), and we found that the smaller the value of Δz , the higher is the emission peak after
5 urine application and smaller are the emission peaks in the following days. Firstly, this is caused
6 by a smaller value of R_{soil} , due to the thinner source layer. Secondly, since the thinner layer can
7 store less TAN in total, the source layer runs out of TAN more quickly leading to lower peaks
8 in the later part of the modelling period.

9 In addition, we carried out a simulation with the maximum value of Δz , the penetration depth
10 of incoming urine. Considering that the water content of a y dm thick soil layer can be expressed
11 as $A_{\text{patch}} \times y \times (\theta_{\text{fc}} - \theta_{\text{ppw}})$, the urine deposited in a single patch (W_{urine}) in this experiment will
12 fill up a $y = 0.2$ dm = 20 mm thick soil layer. In this case, R_{soil} is at least 5 times higher than in
13 the original run (or even bigger as there is more water in the source layer consequently, the
14 layer dries out more slowly), that prevents NH_3 from escaping from the soil shortly after urine
15 deposition. However, from the second day due to the higher available TAN budget, the fluxes
16 are closer to the measurements.

17 **By**In contrast to Δz , the model does not appear to be very sensitive to A_{patch} , with even a +20%
18 change causing less than 2% change in total emission (Table 45). Laubach et al. (2012)
19 estimated that the patches gradually grew by lateral diffusion, so that the area of the patches
20 had doubled over the modelling period at the ~~validation measurement~~ site. Therefore, we
21 conducted a simulation with GAG with a gradually growing patch, whose area doubles by the
22 end of the period. In Fig. 7 we show the measured emission fluxes in relation to constant and
23 gradually increasing values of A_{patch} , with the model results expressed for the whole area ($F_e(t_i)$
24 ~~$= F_e^{\text{single}}(t_i) \times (156 \times A_{\text{patch}}(t_i)) / 804.9$~~); converted based on the reorganized form of Eq. 55).

25 The largest difference with the growing patches, compared with the original run, occurred over
26 the first two days. Then, the emission rates became smaller for the growing patches than with
27 the constant patch area. The difference is a consequence of the combined effect of the growing
28 source area ($156 \times A_{\text{patch}}(t_i)$) and the changing emission flux from a single patch.

29 In our model if a urine patch grows, it means physically that the initial liquid content is diffusing
30 in the soil horizontally, leading to gradually declining volumetric water content. In addition,
31 the evaporating area grows simultaneously, further intensifying the decrease of water content.
32 Thus, R_{soil} will be smaller, allowing stronger NH_3 emissions in the first two days. This leads to

1 lower TAN budget in the second half of the period, resulting in slightly smaller emissions than
2 in the original run.

3 Finally, it has to be pointed out that we neglect an effect where the presence of hippuric acid in
4 urine may increase urea hydrolysis and consequently, NH₃ emission (Whitehead et al., 1989).
5 Whitehead et al. found that ignoring this triggering effect can lead to up to -10% difference in
6 the cumulative NH₃ volatilization (expressed as the proportion of the total nitrogen content of
7 urine) compared to real urine containing the same amount of urinary N.

8 In the measurement campaign (Laubach et al. 2012) an artificial urine solution was spread on
9 the experimental plot that was enriched with additional urea, so we compared a urea based
10 model with a concentrated urea solution. Therefore, the difference in modelled and measured
11 NH₃ fluxes, originating from this simplification, is possibly negligible, though it could be
12 relevant if the model is applied in real grazing situation. However, Whitehead et al (1989)
13 reported comparable differences in NH₃ emissions when they compared urea+hippuric acid
14 solutions with different total N contents as well as different hippuric acid ratios.

15 The N content of urine ranges widely, not just amongst different animals, but also for different
16 urination events by the same animal (Betteridge et al., 1986 and Hoogendoorn et al., 2010).
17 This means that assuming an average N concentration of 8 g, according to Whitehead et al.
18 (1989) can result in a 10% overestimation in the cumulative volatilization of ammonia if the
19 real nitrogen concentration was as low as 2 g/l. Similarly, in the case of the different ratios of
20 hippuric acid and urea: if we assume that the hippuric acid N is an average of 0.8% of the urea
21 N (based on the data published by Dijkstra et al. (2013) this proportion varies between 1.4 -
22 0.36%), according to Whitehead et al. (1989), the overestimation of the cumulative ammonia
23 emission can be 10% if the proportion of hippuric acid was minimal in reality.

24 As the effect of hippuric acid on urea hydrolysis is not widely investigated in the literature, at
25 the moment the current approach is the best we can achieve to simulate the decomposition
26 chemistry in urine. Although the field scale model would most likely underestimate ammonia
27 emission due to the exclusion of the effect influence of hippuric acid, this underestimation may
28 be partly balanced by the sources of overestimation in the model. Nonetheless, this uncertainty
29 should be addressed when the model is applied on field scale.

1 5.3 Uncertainties in the estimation of soil pH

2 The main uncertainty in the model pH calculation is the applied buffering capacity (β).
3 Apparently, the model is not highly sensitive to the tested changes of β ; however, using the
4 same β for every soil type could lead to errors in NH_3 emission estimation. Therefore, we tested
5 the model with two contrasting assumptions about buffering capacity: a) when the system is
6 totally buffered (pH is constant) and b) when there is not any buffering effect ($\beta = 0$). For the
7 constant pH scenario, we chose the soil pH measured before the deposition of the urine patches
8 (pH=6.65).

9 The results show (Fig. 8) that with a constant soil pH, GAG fails to capture the first, dominant
10 peak in emission. This suggests that ~~online~~dynamic modelling of pH is necessary for a proper
11 estimation of NH_3 emission. By contrast, with $\beta = 0$ the model overestimates the first emission
12 peak, while there is little difference in NH_3 fluxes in the rest of the period. Thus, with $\beta = 0$ the
13 model is still capable of reproducing the daily cycle of NH_3 emission.

14 Another feature of the model which affects the pH as well as the emission flux calculation is
15 the handling of CO_2 emission following urine deposition (as discussed in Section 2.6). ~~This is~~
16 ~~also suggested by the~~ sudden drop ~~can be seen in the~~ simulated pH at the beginning of the
17 rain event (Fig. ~~4 (b))4b~~), which ~~seemstends~~ to disappear if there is no rainfall over the
18 modelling period (Fig. ~~9 (a))9a~~, blue line).

19 At the beginning of the rainfall the volume of the gaseous part of the model soil pore suddenly
20 shrinks as the liquid part grows with the incoming water. As a result (given that the base model
21 does not allow CO_2 emission), gaseous CO_2 accumulates in the soil pore and is forced to
22 dissolve into the liquid phase. This intensifies the formation of carbonic acid and its subsequent
23 dissociation, leading to significant drop in pH.

24 In the experiment by Wang et al. (2013) CO_2 emission over urine patches peaked within 8 hours
25 after urine application, while both Ma et al. (2006) and Lin et al. (2009) found that the first peak
26 of CO_2 emission occurred on the first day. In addition, Lin et al. (2009) reported a high
27 correlation ($r=0.63$) between CO_2 emission and soil temperature, suggesting a strong
28 temperature dependency (similarly, we found a correlation of 0.58 for NH_3 , see Table ~~7-6~~).

29 Based on the above similarities between the temporal development of NH_3 and CO_2 emission,
30 to test the effect of CO_2 emission on the GAG simulations, we assumed that the amount of
31 emitted CO_2 is half of the emitted NH_3 in moles (similarly to urea hydrolysis where from one

1 urea molecule two NH_4^+ and one HCO_3^- ions are produced). Even if this is a simplification for
2 CO_2 emission, the results show the potential of future more comprehensive incorporation of the
3 process into the model. By accounting for CO_2 emission the modelled pH values were found to
4 be closer to the measured ones, while the sudden drop at the start of the rain event also largely
5 disappeared (Fig. 9). As a consequence of these changes, the NH_3 emission fluxes were larger
6 before the second day and - due to the larger loss in TAN budget - were smaller in the latter
7 part of the experiment.

8 The apparently contradictory results with the assumed CO_2 emission above - better agreement
9 in pH and poorer agreement in the NH_3 fluxes - suggest that the TAN in the model soil pore is
10 depleted too early, leading to a significant underestimation of the emission fluxes in the second
11 part of the modelling period. Two scenarios can be envisaged that could cause this effect:
12 scenario 1) the simulated rate of urea hydrolysis is higher than it is in reality, or scenario 2) at
13 the experimental site fresh urea that had been intercepted by leaves and dried onto leaf surfaces,
14 was washed to the soil during the rain event, thereby maintaining NH_3 emission afterwards.

15 As we discussed in Section 4, the measurement data also suggest the feasibility of scenario 2.
16 Therefore, we tested the model - assuming that 10% of the applied urine was intercepted on the
17 leaf surface - with 1.5 g of urea washed in during the rain event (see Section [SSS4](#) in the
18 supplementary material). ~~The simulation resulting from~~With this assumption ~~is consistent~~
19 modelled values were in better agreement with observations not only in the case of NH_3
20 exchange flux (Fig. 10d) but also the TAN budget and soil pH (see both at Fig. S2). These
21 results clearly support the idea of the possible restart of breakdown of the fresh urea penetrating
22 to the soil dissolved in rain water ~~(for emission flux see Fig. 10 d in Section 6, for TAN budget~~
23 ~~and pH see Fig. S2).~~

Formatted: Subscript

Formatted: Font: Times New Roman, Not Bold

24 **5.4 Uncertainties in the estimation of the water budget**

25 The GAG model is found to be sensitive to model constants related to the water budget,
26 especially field capacity, θ_{fc} (Table [45](#)). The high sensitivity to a low value of θ_{fc} appears to be
27 because this limits the amount of urine which remains available for hydrolysis and NH_3
28 emission from the source layer. In addition, we also found large differences in total ammonia
29 emission when we modified the permanent wilting point. On regional scale it is not likely to
30 have a database of measured θ_{fc} and θ_{pwp} values over a dense grid. It is more feasible that a soil
31 texture map can be used for this purpose with recommended values of θ_{fc} and θ_{pwp} values for

1 different soil types. Both θ_{fc} and θ_{pwp} can have an uncertainty of $\pm 20\%$ (e.g. in Allen et al.
2 (1998) for sandy loam $\theta_{fc}=0.18-0.28$), similarly to the extent of modification in the current
3 sensitivity test. Therefore, at regional application, this uncertainty has to be considered when
4 interpreting the model results.

5 In addition, a limitation of the calculation of the water budget is that GAG does not account for the
6 water movement in the soil, including the effect of capillary force, diffusion of water in the soil as
7 well as the concentration of TAN and urea within the moving liquid. However, the simulation of
8 these processes is very complex. Shorten and Pleasants (2007) published a system of partial
9 differential equations describing these processes, which could be a basis for further development of
10 GAG.

11

12 **6 Sensitivity to meteorological factors**

13 For quantitative comparison, we show a variety of meteorological factors and the hourly NH_3
14 emission fluxes in Fig. 10. The NH_3 emission flux peaks almost every day shortly after midday,
15 when soil temperature reaches its maximum. The only exception is the second day after urine
16 application when the curve of emission flux stayed flat in the simulation, which was linked to
17 the rain event as discussed in the previous sections.

18 The close relationship between the soil as well as the air temperature and NH_3 emission fluxes
19 can be also seen in the calculated high correlations ($r=0.58$ and $r=0.60$, respectively). Compared
20 with the other meteorological factors (Table 5) the relationship with these two seems to be the
21 strongest. Relative humidity apparently has a slightly weaker, but still considerable role in the
22 simulated NH_3 volatilization ($r=-0.49$). Based on the correlation values, there was a weaker
23 relationship with wind speed ($r=0.40$), which may be related to the fact that simulated R_{soil}
24 provided a much larger constraint on NH_3 soil emission than the atmospheric resistances (Fig.
25 5). Global radiation as well as atmospheric pressure indicated a weaker influence (lower than
26 $r=0.40$ in absolute value) on the simulated NH_3 emission.

27 We also carried out a sensitivity analysis to the different meteorological parameters. To test the
28 sensitivity to a given parameter, we modified it, while keeping all the other parameters the
29 same, we ran a simulation with GAG. At the end of every simulation we calculated the total
30 ammonia emission over the period, and expressed it as the percentage difference compared to
31 the total emission in the original run. To get comparable results, we modified the original

1 datasets in every case by $\pm \Delta x$, calculated as 10% of the difference between the measured
2 minimum and maximum value of the given parameter over the modelling period.

3 Table 56 shows that NH_3 emission is the most sensitive to relative humidity (the differences in
4 total emission were +9.1% and -8.6%) and wind speed (the differences were -5.5% and 4.7%).
5 In addition, a relatively high difference (+4.1%) was observed in the case of global radiation
6 when its values were raised by Δx .

7 In spite of the high correlations, when soil and air temperature were modified separately, we
8 got relatively small anomalies in the total emissions (less than 3% in absolute value for both
9 soil and air temperature). However, when air and soil temperature were adjusted together
10 (assuming that the change of these two temperature parameters is parallel), the differences were
11 larger (see Table 56). Only low sensitivity was detected in the case of atmospheric pressure and
12 hourly precipitation.

13 The results for wind speed and the different temperature parameters can be easily explained.
14 Wind plays a governing role in turbulent mixing of the quasi-laminar and turbulent layer;
15 consequently, it has a considerable effects on the vertical atmospheric transfer of ammonia.
16 Regarding temperature, urea hydrolysis as well as the compensation point both in the stomata
17 and the soil pores follow an exponential function of temperature.

18 Sutton et al. (2013) used a metric, Q_{10} , to express the relative increase in NH_3 emission over a
19 range of 10°C . ~~The combined temperature sensitivity presented in Table 5 amounts to around
20 3.31% change in emission per $^\circ\text{C}$ ($Q_{10}=1.0331$). Based on that $Q_{10} = Q_1^{10}$, according to our
21 simulations, for a urine patch Q_{10} is going to be approximately 1.39. This value is rather smaller
22 than the temperature dependencies for many volatilisation situations reviewed by Sutton et al.
23 (2013). In the case of the GAG simulations, this relatively modest temperature response may
24 in part results from altering the rapidity of emission, while constrained by the available TAN
25 pool. We derived Q_{10} by running the model with 10°C higher air and soil temperature. The
26 resulted value of 1.26 compared to that reported by Sutton et al. for grazing (4.7 for sheep sites)
27 suggest a rather modest temperature sensitivity. The model showed similarly modest sensitivity
28 when we tested it with three and five times higher N concentration in urine (allowing more TAN
29 in the later stages of the modelling period) (Table 7). Based on this results it can be concluded
30 that the lower Q_{10} values are not a consequence of the limited TAN available in the later stages
31 of the modelling period.~~

Formatted: Subscript

1 A possible explanation for the difference between the reported and the simulated temperature
2 sensitivity can be the temporal development of Q_{10} over time (Fig. 11). We calculated the Q_{10}
3 values for every time step as the ratio of the cumulative emissions from the higher temperature
4 model version and the original one, and we found that NH_3 emission is more sensitive to
5 temperature in the first six hours than in the later stages. Considering, that over a grazed field
6 urine patches are deposited in every time step, creating a peak in the individual patch emissions,
7 the total emission for the whole field will be presumably more sensitive to temperature than
8 that for a single urine patch.

9 RH has a dual effect on NH_3 emission. Firstly, it plays a vital role in the water budget and
10 secondly, it also influences the deposition of ammonia to the leaf surface. We tested the
11 sensitivity in a model scenario where relative humidity was modified only in evaporation, and
12 we observed only a +3.2% difference for $-\Delta x$ and -2.8% for $+\Delta x$ change. This clearly suggests
13 that the effect of RH on NH_3 emission in GAG is stronger through deposition to leaf surfaces
14 than through soil evaporation.

15 The physical explanation for the opposite change in RH and the total emission is that at higher
16 values of relative humidity the formation of a water film on the leaf surface is more likely. As
17 a result, deposition is more effective (see the different fluxes in Fig. S1), which will generate a
18 loss in the net emission flux over the whole system (including the exchange with soil and
19 stomata as well as the deposition to cuticle).

20 Although precipitation was shown to suppress modelled emission, the total emission over the
21 period was not strongly sensitive to a change of $\pm 10\%$ (± 0.08 mm) (Table ~~6~~). This is a result
22 of the model features that 1) allow only a $(\Delta z \times (\theta_{fc} - \theta_{pwp})) = 1.2$ mm of maximum liquid content
23 in the model soil pore and 2) do not allow wash out TAN from the source layer. Therefore, in
24 the GAG model even a heavy rain event (> 6 mm / hr) - apart from the slight effect on
25 evaporation - has the same effect as a modest 1.2 mm / hr of precipitation. In the ~~validation~~
26 ~~experiment~~ test simulation during the rain event the soil reached its maximum water content
27 (θ_{fc}). We found that by decreasing the amount of total precipitation so that the soil does not
28 reach θ_{fc} , the maximum difference in total emission was +3%.

29 In addition, the timing of the rain event can also lead to a difference in total NH_3 emission due
30 to the associated increase in R_{soil} which tends to suppress the rate of volatilization. We found
31 that the timing of the rain event affects the NH_3 emission, with up to a 6% reduction or 2%
32 increase in the total NH_3 emission (see the model results in Section ~~S6S5~~). Nevertheless, it must

1 be emphasized that in reality NH_3 can escape from wet soil not only through gaseous diffusion
2 in the empty soil pores. Dissolved NH_3 may get to the soil surface also through the solution and
3 can be volatilized from there (Cooter et al., 2010). This is not taken into account in the present
4 soil resistance parametrisation. Therefore, the effect of rainfall might not be as strong as this
5 experiment showed. On the other hand, as we mentioned earlier, during a dry period urea
6 hydrolysis may slow or stop in absence of water. If the rainfall begins after such a dry period,
7 by restarting urea hydrolysis, it can even enhance ammonia emission rather than
8 ~~supress~~suppress it.

9

10 7 Discussion

11 ~~7.1 Conclusiones~~

12 We constructed a novel NH_3 emission model for a urine patch (GAG) that is capable of
13 simulating the TAN and the water content of the soil under a urine patch and also soil pH.
14 ~~According to the model validation, these are well represented by the model.~~ The difference
15 between the simulated and measured values suggested that to improve the model, further
16 investigation is needed regarding the effect of a possible restart of urea hydrolysis with rain
17 events.

18 The sensitivity analysis to the uncertain parameters showed that soil resistance had more than
19 an order of magnitude stronger effect on soil NH_3 emission than the atmospheric resistances.
20 An exceptional case is when weak wind is coupled with dry soil, in which case atmospheric
21 and soil resistances may become comparable.

22 Our sensitivity analysis also showed that if the thickness of the source layer (Δz) is modified
23 by a given percentage, the difference in the resulting total ammonia emission over the modelling
24 period will be half of this percentage. Therefore, this source of error must be considered when
25 model results are evaluated. Future work should also consider how independent datasets can
26 help characterize the depth of the effective soil emission layer, as well as consider how both
27 downward and upward migration of TAN with deeper soil layers can be addressed.

28 In the case of pH we showed that process-based modelling of pH is necessary to reproduce the
29 very first high peak in NH_3 emission. The simulations were carried out with an assumed soil
30 buffering capacity. While this affects the timing of emissions, we found that the total emission

1 is not sensitive to the value of β and it is able to represent the main temporal development of
2 ammonia emission even with 0 buffering capacity.

3 On the other hand, we found that incorporating a simple ~~estimate~~estimation of CO₂ emission
4 allows the model to reproduce the measured soil pH values more accurately than neglecting
5 CO₂ emissions. Future work should therefore consider how CO₂ fluxes could be incorporated
6 more systematically into the GAG model.

7 The model turned out to be sensitive to the value of soil water content at field capacity (θ_{fc}) and
8 at permanent wilting point (θ_{pwp}). Thus, at regional scale application, where mostly
9 recommended values of these parameters are available, this error has to be considered when
10 interpreting the model results.

11 Our results support the vital role of temperature in NH₃ exchange, showing a high correlation
12 with the temperature parameters as well as strong sensitivity to them. Nevertheless, the GAG
13 model provides only a modest overall temperature dependence in total NH₃ emission compared
14 ~~with a review for several other surface types (Sutton et al., 2013). While temperature is clearly~~
15 ~~important in controlling diurnal dynamics within GAG, the overall emission rate is partly~~
16 ~~constrained by the TAN budget to what was reported in the literature earlier. A possible~~
17 ~~explanation for this is that, according to our results, the sensitivity to temperature is higher close~~
18 ~~to urine application than in the later stages and may depend also on interactions with other~~
19 ~~nitrogen cycling processes.~~

20 In addition, we found that wind speed and relative humidity are also significant influencing
21 factors. In the case of RH we observed a dual effect through its effect on the modelled soil
22 evaporation and the modelled deposition to leaf surfaces, with the latter being the dominant
23 term for the present simulations.

24 ~~As~~In contrast to the NH₃ volatilization models published earlier for urea affected soils (Sherlock
25 and Goh, 1985; Rachhpal and Nye, 1986), our model ~~incorporates, incorporating~~ a canopy
26 compensation point model ~~it,~~ accounts for the effect of the meteorological parameters,
27 providing a more realistic estimation for NH₃ on net canopy exchange ~~than the earlier NH₃~~
28 volatilization models for urea affected soils (Sherlock and Goh, 1985, Rachhpal and Nye,
29 1986) of NH₃. Compared ~~to~~with the model constructed by Laubach et al. (2012), GAG is
30 capable of simulating the influence of vegetation on NH₃ exchange. In addition, our model also
31 simulates soil pH, the TAN and the water content of the soil, allowing it to predict net NH₃

1 emission, instead of operating only in ~~“inverse”~~“inverse” mode, calculating soil parameters
2 based on flux measurements.

3 OnlineRachhpal and Nye (1986) suggested a solution for dynamic modelling of soil pH with a
4 set of continuity equations. However, in their approach the dissociation coefficients, as well as
5 the urea hydrolysis rate, were independent of temperature. Even though the GAG model
6 accounts for the same chemical reactions, it incorporates a different mathematical description
7 and accounts for the missing temperature dependencies.

8 Dynamic simulation of soil pH is novel among the NH₃ exchange models on the ecosystem
9 scale. In the PaSim ecosystem model (Riedo et al., 2002) pH is treated as a constant, and the
10 same is true for the VOLT’AIR model (Génermont and Cellier, 1997) developed for simulating
11 NH₃ emission related to fertilizer and manure application. Furthermore, the framework of GAG
12 is simpler and requires less input data than the VOLT’AIR model. Therefore, for grazing
13 situations, it is much easier to adapt GAG on both field and regional scale.

14 As our final goal is to apply the model to regional scale, simplicity was a key aspect of the
15 model development, avoiding extra steps of model simplification in the later stages of our
16 project. Therefore, the model operates with a single layer approach in the soil. Although this is
17 a simpler approach compared to the some of the above mentioned models (Rachhpal and Nye,
18 1986, Génermont and Cellier, 1997 and Riedo et al., 2002), the model code is easily amendable,
19 which enables to add new modules to GAG in the future.

20 Since all the input parameters can be obtained for larger scales, considering the possible errors,
21 GAG is concluded to be suitable for larger scale application, such as in regional atmospheric
22 and ecosystem models. In addition, as it is dynamically driven by weather parameters, it can
23 serve as a base for further studies of climate dependency of ammonia emission from grazed
24 fields on both plot and regional scale.

26 8 Conclusions

27 We report the description of a process-based, weather-driven ammonia exchange model for a
28 urine patch that is capable of simulating the TAN and the water content of the soil under a urine
29 patch and also soil pH.

30 The model tests suggest that ammonia volatilization from a urine patch can be affected by the
31 possible restart of urea hydrolysis after a rain event as well as CO₂ emission from the soil.

Formatted: Not Superscript/ Subscript

1 The vital role of temperature in NH₃ exchange is supported by our model results; however, the
2 GAG model provides only a modest overall temperature dependence in total NH₃ emission
3 compared with the literature. This, according to our findings, can be explained by the higher
4 sensitivity to temperature close to urine application than in the later stages and may depend on
5 interactions with other nitrogen cycling processes. In addition, we found that wind speed and
6 relative humidity are also significant influencing factors. These relationships need to be further
7 tested in relation to field measurements.

8 For simplicity, to allow subsequent regional upscaling, the model operates with a single soil
9 layer approach, neglecting water movement and solution mixing in the soil. Although this is a
10 limitation of the current model version, the model code is easily amendable, which facilitates
11 to add new modules to GAG in the future.

12 Considering that all the input parameters can be obtained for larger scales, GAG is potentially
13 suitable for field and regional scale application, serving as a tool for further investigation of the
14 effects of climate change on ammonia emissions and deposition.

16 **Acknowledgements**

17 This work was carried out within the framework of the ÉCLAIRE project (Effects of Climate
18 Change on Air Pollution and Response Strategies for European Ecosystems) funded by the EU's
19 Seventh Framework Programme for Research and Technological Development (FP7).

21 **Abbreviations**

<u>Abbreviation (unit)</u>	<u>Model variable</u>
$\frac{D_{O_3}}{D_{NH_3}}$	<u>Ratio of diffusivity of O₃ and NH₃</u>
<u>[X] (mol dm⁻³)</u>	<u>Concentration of compound X</u>
<u>a</u>	<u>Parameter for calculating R_w</u>
<u>A_h</u>	<u>Parameter for urea hydrolysis simulation</u>
<u>A_{patch} (m²)</u>	<u>Area of a urine patch</u>

<u>B_C (mol)</u>	<u>Carbon content of the source layer (originating from urea)</u>
<u>B_{H_2O} (dm³)</u>	<u>Water budget in the source layer</u>
<u>$B_{H_2O(max)}$ (dm³)</u>	<u>Maximal water amount in the source layer</u>
<u>$B_{H_2O(min)}$ (dm³)</u>	<u>Minimal water amount in the source layer</u>
<u>$B_{H_2O}^*$ (dm³)</u>	<u>Precalculated water budget in the source layer</u>
<u>$B_{H_2O}^{Tot}$ (dm³)</u>	<u>Total water budget under a urine patch</u>
<u>B_N (mol)</u>	<u>TAN + gaseous ammonia content in the source layer</u>
<u>B_{TAN} (g N)</u>	<u>TAN budget in the source layer</u>
<u>B_{urea} (g N)</u>	<u>Urea budget under a urine patch</u>
<u>B_X (mol) (X= H_2CO_3, HCO_3^-, CO_3^{2-}, $CO_{2(g)}$, NH_4^+, $NH_{3(aq)}$, $NH_{3(g)}$, H^+)</u>	<u>Budget of a chemical compound X under the urine patch</u>
<u>C_d</u>	<u>Effect of day and night on evapotranspiration</u>
<u>c_N (N dm⁻³)</u>	<u>N content of the urine</u>
<u>c_N^{Tot} (g N dm⁻³)</u>	<u>Urine N content after dilution in the soil</u>
<u>D_g (m² s⁻¹)</u>	<u>Diffusivity of NH₃ in air</u>
<u>E (mm h⁻¹)</u>	<u>Soil evaporation rate</u>
<u>e_a (kPa)</u>	<u>Actual water vapour pressure</u>
<u>e_s (kPa)</u>	<u>Saturated water vapour pressure</u>
<u>ET (mm h⁻¹)</u>	<u>Actual evapotranspiration rate</u>
<u>ET_0 (mm h⁻¹)</u>	<u>Reference evapotranspiration rate</u>
<u>f_c (m² m⁻²)</u>	<u>Vegetation coverage</u>
<u>F_f (μg N m⁻² s⁻¹)</u>	<u>NH₃ exchange flux with the foliage</u>
<u>F_g (μg N m⁻² s⁻¹)</u>	<u>NH₃ exchange flux over the ground</u>

E_{sto} ($\mu\text{g N m}^{-2} \text{s}^{-1}$)	<u>NH₃ exchange flux with stomata</u>
E_t ($\mu\text{g N m}^{-2} \text{s}^{-1}$)	<u>Total NH₃ exchange flux over the canopy</u>
f_w ($\text{m}^2 \text{m}^{-2}$)	<u>Wetted uncovered soil fraction</u>
E_w ($\mu\text{g N m}^{-2} \text{s}^{-1}$)	<u>NH₃ deposition flux to water and waxes on the leaf surface</u>
G ($\text{MJ m}^2 \text{h}^{-1}$)	<u>Soil heat flux</u>
g_{light}	<u>Relative conductance for the effect of light on g_s</u>
g_{max} ($\text{mmol O}_3 \text{m}^{-2}$)	<u>Maximal stomatal conductance</u>
g_{min}	<u>Minimal relative stomatal conductance</u>
g_{pot}	<u>Relative stomatal conductance for the effect of plant phenological state on g_s</u>
g_s ($\text{mmol O}_3 \text{m}^{-2}$)	<u>Stomatal conductance for O₃</u>
g_{SWP}	<u>Relative conductance for the effect of soil water on g_s</u>
g_{temp}	<u>Relative conductance for the effect of temperature on g_s</u>
g_{VPD}	<u>Relative conductance for the effect of vapour pressure deficit on g_s</u>
$H(X)$ ($\text{mol dm}^{-3} (\text{mol dm}^{-3})^{-1}$)	<u>Henry coefficient for the given gas X</u>
i_C (mol)	<u>Carbon input to the urine patch</u>
i_N (mol)	<u>TAN input to the urine patch (TAN production in moles)</u>
$K(X)$ (mol dm^{-3})	<u>Dissociation constant for the given compound X</u>
K_c	<u>Crop coefficient</u>
K_{cb}	<u>Transpiration coefficient</u>
K_e	<u>Soil evaporation coefficient</u>
K_h	<u>Urea hydrolysis constant</u>

<u>L (m)</u>	<u>Monin-Obukhov length</u>
<u>LAI (m² m⁻²)</u>	<u>Leaf area index</u>
<u>N_{app} (kg N ha⁻¹)</u>	<u>Nitrogen applied over a urine patch</u>
<u>N_{prod} (g N)</u>	<u>TAN production</u>
<u>P (mm)</u>	<u>Precipitation</u>
<u>PAR (μmol m² s⁻¹)</u>	<u>Photosynthetically active radiation</u>
<u>R_a (s m⁻¹)</u>	<u>Aerodynamic resistance over the canopy</u>
<u>R_{ac} (s m⁻¹)</u>	<u>Aerodynamic resistance in the canopy</u>
<u>R_b (s m⁻¹)</u>	<u>Resistance of the quasi-laminar layer over the canopy</u>
<u>R_{bg} (s m⁻¹)</u>	<u>Resistance of the quasi-laminar layer in the canopy</u>
<u>REW (mm)</u>	<u>Readily evaporable water in the soil</u>
<u>R_{glob} (MJ m²h⁻¹)</u>	<u>Global radiation / solar radiation</u>
<u>RH (%)</u>	<u>Relative humidity</u>
<u>R_n (MJ m² h⁻¹)</u>	<u>Net radiation</u>
<u>r_{RX} (mol)</u>	<u>Consumption or production of a given compound in reaction X.</u>
<u>R_{soil} (s m⁻¹)</u>	<u>Soil resistance</u>
<u>R_{sto} (s m⁻¹)</u>	<u>Stomatal resistance</u>
<u>R_{sto}(O₃)(s m⁻¹)</u>	<u>Stomatal resistance for O₃</u>
<u>R_w (s m⁻¹)</u>	<u>Cuticular resistance</u>
<u>R_w(min) (s m⁻¹)</u>	<u>Minimal cuticular resistance</u>
<u>S_{MI}</u>	<u>Soil moisture index</u>
<u>T (°C)</u>	<u>Air temperature at 2 m</u>
<u>t_i</u>	<u>ith time step</u>
<u>T_{soil} (°C)</u>	<u>Soil temperature</u>

u ($m s^{-1}$)	<u>Wind speed</u>
u^* ($m s^{-1}$)	<u>Friction velocity</u>
u^*g	<u>Friction velocity at ground level in the canopy</u>
U_{add} ($g N$)	<u>Urea added to the source layer</u>
V_{air} (dm^3)	<u>Volume of the air in the source layer</u>
W_{evap} (dm^3)	<u>Water loss as soil evaporation from the urine patch</u>
W_{rain} (dm^3)	<u>Water input as rain water over the urine patch</u>
W_{urine} (dm^3)	<u>Volume of urine</u>
z_l (m)	<u>Height of the top of logarithmic wind profile</u>
z_w (m)	<u>Height of wind measurement</u>
α	<u>Parameter for calculating R_{ac}</u>
β ($mol H^+ (pH unit)^{-1} dm^{-3}$)	<u>Soil buffering capacity</u>
β_{patch} ($mol H^+ (pH unit)^{-1}$)	<u>Buffering capacity of the source layer</u>
γ ($kPa ^\circ C^{-1}$)	<u>Psychometric constant</u>
Γ_p	<u>NH_3 emission potential in the soil pore</u>
Γ_{sto}	<u>NH_3 emission potential from the stomata</u>
$\Gamma_{sto(max)}$	<u>Maximal NH_3 emission potential from the stomata</u>
Δ ($kPa ^\circ C^{-1}$)	<u>Slope of saturation vapour pressure curve</u>
Δz (mm)	<u>Thickness of the source layer</u>
Δz_E (m)	<u>Thickness of the evaporation layer</u>
θ ($m^3 m^{-3}$)	<u>Volumetric water content</u>
θ_{fc} ($m^3 m^{-3}$)	<u>Field capacity</u>
θ_{por} ($m^3 m^{-3}$)	<u>Porosity</u>
θ_{pwp} ($m^3 m^{-3}$)	<u>Permanent wilting point</u>
ξ	<u>Soil tortuosity</u>

τ (days)	Decay parameter
χ_a ($\mu\text{g N m}^{-3}$)	Air concentration of NH_3
χ_c ($\mu\text{g N m}^{-3}$)	Compensation point above the vegetation
χ_p ($\mu\text{g N m}^{-3}$)	Compensation point in the soil pores
χ_{sto} ($\mu\text{g N m}^{-3}$)	Stomatal compensation point
χ_{z0} ($\mu\text{g N m}^{-3}$)	Canopy compensation point

1

2 References

3 Allen, R. G., Pereira, L. S., Raes, D. and Smith, M.: Crop evapotranspiration-Guidelines for
4 computing crop water requirements, FAO Irrigation and drainage paper 56, FAO, Rome, Italy,
5 1998.

6 [Bates, R. G. and Pinching, G. D.: Acidic dissociation constant of ammonium ion at 0-degrees-](#)
7 [C to 50-degrees-C, and the base strength of ammonia, J. Res. Nat. Bur. Stand., 42, 419-430,](#)
8 [doi:10.6028/jres.042.037, 1949.](#)

9 [Betteridge, K., Andrewes, W. G. K. and Sedcole, J. R.: Intake and excretion of nitrogen,](#)
10 [potassium and phosphorus by grazing steers, J Agr Sci, 106, 393-404, 1986.](#)

11 [Burkhardt, J., Kaiser, H., Goldbach, H. and Kappen, L.: Measurements of electrical leaf surface](#)
12 [conductance reveal re-condensation of transpired water vapour on leaf surfaces, Plant, Cell](#)
13 [Environ., 22, 189-196, doi:10.1046/j.1365-3040.1999.00387.x, 1999.](#)

14 Burkhardt, J., Flechard, C. R., Gresens, F., Mattsson, M., Jongejan, P. A. C., Erisman, J. W.,
15 Weidinger, T., Meszaros, R., Nemitz, E. and Sutton, M. A.: Modelling the dynamic chemical
16 interactions of atmospheric ammonia with leaf surface wetness in a managed grassland canopy,
17 Biogeosciences, 6, 67-84, [doi:10.5194/bg-6-67-2009](#), 2009.

18 Cooter, E. J., Bash, J. O., Walker, J. T., Jones, M. R. and Robarge, W.: Estimation of NH_3 bi-
19 directional flux from managed agricultural soils, Atmos. Environ., 44, 2107-2115,
20 [10.1016/j.atmosenv.2010.02.044](#), 2010.

1 [Dasgupta, P. K. and Dong, S.: Solubility of ammonia in liquid water and generation of trace](#)
2 [levels of standard gaseous ammonia, *Atmos. Environ.*, 20, 565-570, doi:10.1016/0004-](#)
3 [6981\(86\)90099-5, 1986.](#)

4 [Dijkstra, J., Oenema, O., van Groenigen, J. W., Spek, J. W., van Vuuren, A. M. and Bannink,](#)
5 [A.: Diet effects on urine composition of cattle and N₂O emissions, *animal*, 7, 292-302,](#)
6 [doi:10.1017/S1751731113000578, 2013.](#)

7 Doak, B. W.: Some chemical changes in the nitrogenous constituents of urine when voided on
8 pasture, *J Agr Sci*, 42, 162-171, 1952.

9 EDGAR: Emissions Database for Global Atmospheric Research v4.2,
10 <http://edgar.jrc.ec.europa.eu/>, last access: 20 May 2014, 2011.

11 Emberson, L., Simpson, D., Tuovinen, J.-P., Ashmore, M. and Cambridge, H.: Towards a
12 model of ozone deposition and stomatal uptake over Europe, EMEP MSC-W Note 6/2000, The
13 Norwegian Meteorological Institute, Oslo, Norway, 2000.

14 Farquhar, G. D., Firth, P. M., Wetselaar, R. and Weir, B.: On the Gaseous Exchange of
15 Ammonia between Leaves and the Environment: Determination of the Ammonia
16 Compensation Point, *Plant. Physiol.*, 66, 710-714, [doi:10.1104/pp.66.4.710](#), 1980.

17 Flechard, C. R., Fowler, D., Sutton, M. A. and Cape, J. N.: A dynamic chemical model of bi-
18 directional ammonia exchange between semi-natural vegetation and the atmosphere, *Q. J. Roy.*
19 *Meteor. Soc.*, 125, 2611-2641, [doi:10.1002/qj.49712555914](#), 1999.

20 Flechard, C. R., Massad, R. S., Loubet, B., Personne, E., Simpson, D., Bash, J. O., Cooter, E.
21 J., Nemitz, E. and Sutton, M. A.: Advances in understanding, models and parameterizations of
22 biosphere-atmosphere ammonia exchange, *Biogeosciences*, 10, 5183-5225, [doi:10.5194/bg-10-](#)
23 [5183-2013](#), 2013.

24 Fowler, D., Coyle, M., Skiba, U., Sutton, M. A., Cape, J. N., Reis, S., Sheppard, L. J., Jenkins,
25 A., Grizzetti, B., Galloway, J. N., Vitousek, P., Leach, A., Bouwman, A. F., Butterbach-Bahl,
26 K., Dentener, F., Stevenson, D., Amann, M. and Voss, M.: The global nitrogen cycle in the
27 twenty-first century, *Philos. T. R. Soc. B*, 368, [20130164](#), [doi:10.1098/rstb.2013.0164](#), 2013.

28 Galloway, J. N., Townsend, A. R., Erismann, J. W., Bekunda, M., Cai, Z., Freney, J. R.,
29 Martinelli, L. A., Seitzinger, S. P. and Sutton, M. A.: Transformation of the Nitrogen Cycle:

1 Recent Trends, Questions, and Potential Solutions, *Science*, 320, 889-892,
2 [doi:10.1126/science.1136674](https://doi.org/10.1126/science.1136674), 2008.

3 Géniermont, S. and Cellier, P.: A mechanistic model for estimating ammonia volatilization from
4 slurry applied to bare soil, *Agr. Forest Meteorol.*, 88, 145-167, ~~1997~~, [doi:P10.1016/S0168-1923\(97\)00044-0](https://doi.org/10.1016/S0168-1923(97)00044-0), 1997.

5 [Harned, H. S. and Davis, R.: The Ionization Constant of Carbonic Acid in Water and the Solubility of Carbon Dioxide in Water and Aqueous Salt Solutions from 0 to 50°, *J. Am. Chem. Soc.*, 65, 2030-2037, doi:10.1021/ja01250a059, 1943.](https://doi.org/10.1021/ja01250a059)

6 [Harned, H. S. and Scholes, S. R.: The Ionization Constant of HCO₃⁻ from 0 to 50°, *J. Am. Chem. Soc.*, 63, 1706-1709, doi:10.1021/ja01851a058, 1941.](https://doi.org/10.1021/ja01851a058)

7
8
9
10

11 Hellsten, S., Dragosits, U., Place, C. J., Vieno, M., Dore, A. J., Misselbrook, T. H., Tang, Y. S.
12 and Sutton, M. A.: Modelling the spatial distribution of ammonia emissions in the UK, *Environ. Pollut.*, 154, 370-379, [doi:10.1016/j.envpol.2008.02.017](https://doi.org/10.1016/j.envpol.2008.02.017), 2008.

13
14 Hicks, B. B., Baldocchi, D. D., Meyers, T. P., Hosker, R. P., Jr. and Matt, D. R.: A preliminary
15 multiple resistance routine for deriving dry deposition velocities from measured quantities,
16 *Water Air Soil Pollut.*, 36, 311-330, [doi:10.1007/BF00229675](https://doi.org/10.1007/BF00229675), 1987.

17 [Hoogendoorn, C. J., Betteridge, K., Costall, D. A. and Ledgard, S. F.: Nitrogen concentration in the urine of cattle, sheep and deer grazing a common ryegrass/cocksfoot/white clover pasture, *New Zeal. J. Agr. Res.*, 53, 235-243, doi:10.1080/00288233.2010.499899, 2010.](https://doi.org/10.1080/00288233.2010.499899)

18
19
20 Horváth, L., Asztalos, M., Führer, E., Mészáros, R. and Weidinger, T.: Measurement of
21 ammonia exchange over grassland in the Hungarian Great Plain, *Agr. Forest Meteorol.*, 130,
22 282-298, [doi:10.1016/j.agrformet.2005.04.005](https://doi.org/10.1016/j.agrformet.2005.04.005), 2005.

23 [Kielland, J.: Individual Activity Coefficients of Ions in Aqueous Solutions, *J. Am. Chem. Soc.*, 59, 1675-1678, doi:10.1021/ja01288a032, 1937.](https://doi.org/10.1021/ja01288a032)

24
25 Laubach, J., Taghizadeh-Toosi, A., Gibbs, S. J., Sherlock, R. R., Kelliher, F. M. and Grover, S.
26 P. P.: Ammonia emissions from cattle urine and dung excreted on pasture, *Biogeosciences*, 10,
27 327-338, [doi:10.5194/bg-10-327-2013](https://doi.org/10.5194/bg-10-327-2013), 2013.

28 Laubach, J., Taghizadeh-Toosi, A., Sherlock, R. R. and Kelliher, F. M.: Measuring and
29 modelling ammonia emissions from a regular pattern of cattle urine patches, *Agr. Forest Meteorol.*, 156, 1-17, ~~2012~~, [doi:10.1016/j.agrformet.2011.12.007](https://doi.org/10.1016/j.agrformet.2011.12.007), 2012.

30

Formatted: German (Germany)

1 Leuning, R., Freney, J. R., Denmead, O. T. and Simpson, J. R.: A sampler for measuring
2 atmospheric ammonia flux, *Atmos. Environ.*, 19, 1117-1124, [doi:10.1016/0004-](https://doi.org/10.1016/0004-6981(85)90196-9)
3 [6981\(85\)90196-9](https://doi.org/10.1016/0004-6981(85)90196-9), 1985.

4 Lin, X., Wang, S., Ma, X., Xu, G., Luo, C., Li, Y., Jiang, G. and Xie, Z.: Fluxes of CO₂, CH₄,
5 and N₂O in an alpine meadow affected by yak excreta on the Qinghai-Tibetan plateau during
6 summer grazing periods, *Soil Biol. Biochem.*, 41, 718-725,
7 [2009,doi:10.1016/j.soilbio.2009.01.007](https://doi.org/10.1016/j.soilbio.2009.01.007), 2009.

8 Ma, X., Wang, S., Wang, Y., Jiang, G. and Nyren, P.: Short-term effects of sheep excrement
9 on carbon dioxide, nitrous oxide and methane fluxes in typical grassland of Inner Mongolia,
10 *New Zeal. J. Agr. Res.*, 49, 285-297, 2006.

11 Massad, R.-S., Tuzet, A., Loubet, B., Perrier, A. and Cellier, P.: Model of stomatal ammonia
12 compensation point (STAMP) in relation to the plant nitrogen and carbon metabolisms and
13 environmental conditions, *Ecol. Model.*, 221, 479-494, [doi:10.1016/j.ecolmodel.2009.10.029](https://doi.org/10.1016/j.ecolmodel.2009.10.029),
14 2010a.

15 Massad, R. S., Nemitz, E. and Sutton, M. A.: Review and parameterisation of bi-directional
16 ammonia exchange between vegetation and the atmosphere, *Atmos. Chem. Phys.*, 10, 10359-
17 10386, [doi:10.5194/acp-10-10359-2010](https://doi.org/10.5194/acp-10-10359-2010), 2010b.

18 Millington, R. J. and Quirk, J. P.: Permeability of porous solids, *T. Faraday Soc.*, 57, 1200-
19 1207, [doi:10.1039/tf9615701200](https://doi.org/10.1039/tf9615701200), 1961.

20 Misselbrook, T. H., Gilhespy, S. L., Cardenas, L. M., Chambers, B. J., Smith, K. A., Williams,
21 J. and Dragosits, U.: Inventory of Ammonia Emissions from UK Agriculture, Inventory
22 Submission Report, DEFRA, [London, UK](https://www.gov.uk/government/uploads/system/uploads/attachment_data/file/234242/Inventory_of_Ammonia_Emissions_from_UK_Agriculture.pdf), 2012.

23 Nemitz, E., Milford, C. and Sutton, M. A.: A two-layer canopy compensation point model for
24 describing bi-directional biosphere-atmosphere exchange of ammonia, *Q. J. Roy. Meteor. Soc.*,
25 127, 815-833, [doi:10.1256/smsqj.57305](https://doi.org/10.1256/smsqj.57305), 2001.

26 Nemitz, E., Sutton, M. A., Schjoerring, J. K., Husted, S. and Paul Wyers, G.: Resistance
27 modelling of ammonia exchange over oilseed rape, *Agr. Forest Meteorol.*, 105, 405-425,
28 [2000,doi:10.1016/S0168-1923\(00\)00206-9](https://doi.org/10.1016/S0168-1923(00)00206-9), 2000.

29 NIWA: The National Climate Database, <http://cliflo.niwa.co.nz/>, last access: 2 December 2013,
30 2015.

1 Petersen, S. O., Sommer, S. G., Aaes, O. and Sørensen, K.: Ammonia losses from urine and
2 dung of grazing cattle: effect of N intake, *Atmos. Environ.*, 32, 295-300, [doi:10.1016/S1352-](https://doi.org/10.1016/S1352-2310(97)00043-5)
3 [2310\(97\)00043-5](https://doi.org/10.1016/S1352-2310(97)00043-5), 1998.

4 [R Core Team: R: A language and environment for statistical computing. R Foundation for
5 Statistical Computing, Vienna, Austria, 2012.](#)

6 Rachhpal, S. and Nye, P. H.: A model of ammonia volatilization from applied urea. I.
7 Development of the model, *J. Soil Sci.*, 37, 9-20, [doi:10.1111/j.1365-2389.1986.tb00002.x](https://doi.org/10.1111/j.1365-2389.1986.tb00002.x),
8 1986.

9 [Riddick, S. N.: Global ammonia emissions from seabird colonies, Ph.D. thesis, Kings College,
10 London, UK, 2012.](#)

11 Riedo, M., Milford, C., Schmid, M. and Sutton, M. A.: Coupling soil–plant–atmosphere
12 exchange of ammonia with ecosystem functioning in grasslands, *Ecol. Model.*, 158, 83-110,
13 [2002-doi:10.1016/S0304-3800\(02\)00169-2](https://doi.org/10.1016/S0304-3800(02)00169-2), 2002.

14 Sherlock, R. R. and Goh, K. M.: Dynamics of ammonia volatilization from simulated urine
15 patches and aqueous urea applied to pasture I. Field experiments, *Fert. Res.*, 5, 181-195,
16 [doi:10.1007/BF01052715](https://doi.org/10.1007/BF01052715), 1984.

17 Sherlock, R. R. and Goh, K. M.: Dynamics of ammonia volatilization from simulated urine
18 patches and aqueous urea applied to pasture. II. Theoretical derivation of a simplified model,
19 *Fert. Res.*, 6, 3-22, [doi:10.1007/BF01058161](https://doi.org/10.1007/BF01058161), 1985.

20 [Shorten, P. R. and Pleasants, A. B.: A stochastic model of urinary nitrogen and water flow in
21 grassland soil in New Zealand. *Agric., Ecosyst. Environ.*, 120, 145-152,
22 \[doi:10.1016/j.agee.2006.08.017\]\(https://doi.org/10.1016/j.agee.2006.08.017\), 2007.](#)

23 Simpson, D., Benedictow, A., Berge, H., Bergström, R., Emberson, L. D., Fagerli, H., Flechard,
24 C. R., Hayman, G. D., Gauss, M., Jonson, J. E., Jenkin, M. E., Nyíri, A., Richter, C., Semeena,
25 V. S., Tsyro, S., Tuovinen, J. P., Valdebenito, Á. and Wind, P.: The EMEP MSC-W chemical
26 transport model; technical description, *Atmos. Chem. Phys.*, 12, 7825-7865, [doi:10.5194/acp-](https://doi.org/10.5194/acp-12-7825-2012)
27 [12-7825-2012](https://doi.org/10.5194/acp-12-7825-2012), 2012.

28 Sutton, M. A. and Fowler, D.: A model for inferring bi-directional fluxes of ammonia over plant
29 canopies, in: WMO Conference on the Measurement and Modeling of Atmospheric
30 Composition Changes including Pollution Transport. WMO/GAW-91, [Sofia, Bulgaria, 04–08
31 October 1993](#), WMO, Geneva, 179-182, 1993.

1 Sutton, M. A., Howard, C. M., Erisman, J. W., Bealey, W. J., Billen, G., Bleeker, A., Bouwman,
2 A. F., Grennfelt, P., van Grinsven, H. and Grizzetti, B.: The challenge to integrate nitrogen
3 science and policies: the European Nitrogen Assessment approach, in: The European Nitrogen
4 Assessment: Sources, Effects and Policy Perspectives, Sutton, M. A., Howard, C. M., Erisman,
5 J. W., Billen, G., Bleeker, A., Grennfelt, P., Van Grinsven, H. & Grizzetti, B. (Eds.), Cambridge
6 University Press, Cambridge, UK, 82-96, 2011.

7 Sutton, M. A., Reis, S., Riddick, S. N., Dragosits, U., Nemitz, E., Theobald, M. R., Tang, Y.
8 S., Braban, C. F., Vieno, M., Dore, A. J., Mitchell, R. F., Wanless, S., Daunt, F., Fowler, D.,
9 Blackall, T. D., Milford, C., Flechard, C. R., Loubet, B., Massad, R., Cellier, P., Personne, E.,
10 Coheur, P. F., Clarisse, L., Van Damme, M., Ngadi, Y., Clerbaux, C., Skj th, C. A., Geels, C.,
11 Hertel, O., Wichink Kruit, R. J., Pinder, R. W., Bash, J. O., Walker, J. T., Simpson, D., Horv th,
12 L., Misselbrook, T. H., Bleeker, A., Dentener, F. and de Vries, W.: Towards a climate-
13 dependent paradigm of ammonia emission and deposition, *Philos. T. R. Soc. B*, 368, [20130166](https://doi.org/10.1098/rstb.2013.0166),
14 [doi:10.1098/rstb.2013.0166](https://doi.org/10.1098/rstb.2013.0166), 2013.

15 Sutton, M. A., Schjorring, J. K. and Wyers, G. P.: Plant-Atmosphere Exchange of Ammonia
16 *Philos. T. R. Soc. A*, 351, 261-276, [doi:10.1098/rsta.1995.0033](https://doi.org/10.1098/rsta.1995.0033), 1995.

17 [Vieno, M., Dore, A. J., Stevenson, D. S., Doherty, R., Heal, M. R., Reis, S., Hallsworth, S.,](#)
18 [Tarrason, L., Wind, P., Fowler, D., Simpson, D. and Sutton, M. A.: Modelling surface ozone](#)
19 [during the 2003 heat-wave in the UK, *Atmos. Chem. Phys.*, 10, 7963-7978, doi:10.5194/acp-](#)
20 [10-7963-2010, 2010.](#)

21 [Vieno, M., Heal, M. R., Hallsworth, S., Famulari, D., Doherty, R. M., Dore, A. J., Tang, Y. S.,](#)
22 [Braban, C. F., Leaver, D., Sutton, M. A. and Reis, S.: The role of long-range transport and](#)
23 [domestic emissions in determining atmospheric secondary inorganic particle concentrations](#)
24 [across the UK, *Atmos. Chem. Phys.*, 14, 8435-8447, doi:10.5194/acp-14-8435-2014, 2014.](#)

25 Walter, I., Allen, R., Elliott, R., Jensen, M., Itenfisu, D., Mecham, B., Howell, T., Snyder, R.,
26 Brown, P., Echings, S., Spofford, T., Hattendorf, M., Cuenca, R., Wright, J. and Martin, D.:
27 ASCE's Standardized Reference Evapotranspiration Equation, in: Watershed Management and
28 Operations Management 2000, American Society of Civil Engineers, [Fort Collins, Colorado,](#)
29 [US, 20-24 June 2000](#), 1-11, 2001.

1 Wang, X., Huang, D., Zhang, Y., Chen, W., Wang, C., Yang, X. and Luo, W.: Dynamic changes
2 of CH₄ and CO₂ emission from grazing sheep urine and dung patches in typical steppe, Atmos.
3 Environ., 79, 576-581, ~~2013~~, doi:10.1016/j.atmosenv.2013.07.003, 2013.

4 Whitehead, D. C., Lockyer, D. R. and Raistrick, N.: Volatilization of ammonia from urea
5 applied to soil: Influence of hippuric acid and other constituents of livestock urine, Soil Biol.
6 Biochem., 21, 803-808, doi:10.1016/0038-0717(89)90174-0, 1989.

7 Whitehead, D. C. and Raistrick, N.: The volatilization of ammonia from cattle urine applied to
8 soils as influenced by soil properties, Plant Soil, 148, 43-51, doi:10.1007/BF02185383, 1993.

9 Wilhelm, E., Battino, R. and Wilcock, R. J.: Low-pressure solubility of gases in liquid water,
10 Chem. Rev., 77, 219-262, doi:10.1021/cr60306a003, 1977.

11 Wu, Y., Walker, J., Schwede, D., Peterslidard, C., Dennis, R. and Robarge, W.: A new model
12 of bi-directional ammonia exchange between the atmosphere and biosphere: Ammonia stomatal
13 compensation point, Agr. Forest Meteorol., 149, 263-280,
14 doi:10.1016/j.agrformet.2008.08.012, 2009.

15
16
17

Formatted: German (Germany)

1 Table 4-1. Chemical equations – indicated by R0-5 - simulated within the model. (where applicable) their equilibrium coefficient according to
 2 definition (K for dissociation and H for dissolution) and the coefficients expressed as the function of soil temperature (T_{soil} (K)) and their
 3 references (squared brackets denotes that the concentration of every compound is in mol dm⁻³).
 4

<u>Chemical equation</u>	<u>Equilibrium coefficient</u>	<u>Equilibrium coefficient as a function of temperature</u>	<u>Reference</u>
<u>R0: $CO(NH_2)_2 + 2H_2O + H^+ \rightarrow 2NH_4^+ + HCO_3^-$</u>	=	=	=
<u>R1: $NH_4^+ \Leftrightarrow NH_{3(aq)} + H^+$</u>	$K(NH_4^+) = \frac{[NH_{3(aq)}][H^+]}{[NH_4^+]}$	$K(NH_4^+) = 5.67 \times 10^{-10} \exp\left(-6286\left(\frac{1}{T_{soil}} - \frac{1}{298.15}\right)\right)$	<u>Bates and Pinching, 1949</u>
<u>R2: $HCO_3^- \Leftrightarrow CO_3^{2-} + H^+$</u>	$K(HCO_3^-) = \frac{[H^+][CO_3^{2-}]}{[HCO_3^-]}$	$\lg(K(X)) = -\left(\left(\frac{a}{T_{soil}}\right) + (b \times T_{soil}) - c\right)$ a=2902.39 b=0.02379 c=6.4980	<u>Harned and Scholes, 1941</u>
<u>R3: $H_2CO_3 \Leftrightarrow HCO_3^- + H^+$</u>	$K(H_2CO_3) = \frac{[HCO_3^-][H^+]}{[H_2CO_3]}$	$\lg(K(X)) = -\left(\left(\frac{a}{T_{soil}}\right) + (b \times T_{soil}) - c\right)$ a=3404.71 b=0.032786 c=14.8435	<u>Harned and Davis, 1943</u>
<u>R4: $NH_{3(aq)} \Leftrightarrow NH_{3(g)}$</u>	$H(NH_{3(g)}) = \frac{[NH_{3(aq)}]}{[NH_{3(g)}]}$	$H(NH_{3(g)}) = 56 \times \exp\left(4092 \times \left(\frac{1}{T_{soil}} - \frac{1}{298.15}\right)\right) \times c_{con}$	<u>Dasgupta and Dong, 1986</u>
<u>R5: $H_2CO_3 \Leftrightarrow CO_{2(g)}$</u>	$H(CO_{2(g)}) = \frac{[H_2CO_3]}{[CO_{2(g)}]}$	$H(CO_{2(g)}) = 0.034 \times \exp\left(2400 \times \left(\frac{1}{T_{soil}} - \frac{1}{298.15}\right)\right) \times c_{con}$	<u>Wilhelm et al., 1977</u>
		<u>(where $c_{con} = \left(\frac{0.001 \frac{m^3}{dm^3} \times 1.013 \times 10^5 \frac{Pa}{atm}}{8.314 \frac{J}{Kmol} \times T_{soil}}\right)^{-1}$ is the conversion from atm (mol dm⁻³)⁻¹ to (mol dm⁻³) (mol dm⁻³)⁻¹)</u>	

5

1 [Table 2](#). Urine patch details from the experiment of Laubach et al. (2012) (or from other
 2 [sources as listed in the footnote](#)) and site specific model constants.

Model constants	Value
Urine patch specific constants	
A_{patch} (area of a urine patch) ¹	0.25 m ²
c_N (N content of the urine)	10 g N dm ⁻³
W_{urine} (volume of urine)	1.5 dm ³
Δz (thickness of the source layer) ²	4 mm
k_h (urea hydrolysis constant) ²³	0.23
Site specific constants	
Longitude	172°27.34'E
Latitude	43°38.56'S
Height above sea level	11 m
θ_{pwp} (permanent wilting point) ³⁴	0.1
θ_{fc} (field capacity) ³⁴	0.4
θ_{por} (porosity)	0.62
f_c (vegetation coverage)	35%
z_w (height of wind measurement)	2.1 m

3 ¹In the experiment the expansion of the patches was observed up to 0.5 m². For model
 4 sensitivity to A_{patch} see Section 5.2.

5 ²² Assumed in this study.

6 ³For summer (Sherlock and Goh, 1984)

7 ²Assumed⁴Assumed based on the provided measured volumetric water content dataset.

8

1 Table 2. ~~Input and validation~~3. Measured data for testing used as input and the base of
 2 ~~comparison with~~ the model results, together with their original time resolution and their
 3 conversion to hourly time resolution.

Variable	Original time resolution	Adaptation to hourly time resolution
Input data		
χ_a ($\mu\text{g N m}^{-3}$)	Various (2-10 hourly)	Interpolated for the required hours.
u (m s^{-1}) – at 2.1 m		
PAR ($\mu\text{mol m}^{-2} \text{s}^{-1}$)		
T _{soil} ($^{\circ}\text{C}$) - at 2 cm	Half hourly	Averaged for the given hour.
p (kPa)		
H ($\text{MJ m}^{-2} \text{h}^{-1}$)		
P (mm)	Half hourly	Summed up for the given hour.
T ($^{\circ}\text{C}$) - at 3.85 m	Half hourly	Averaged for the given hour then calculated to 2 m height considering the average temperature gradient $6.5 \text{ }^{\circ}\text{C/km}$: $T(2\text{m})=T(3.85\text{m})-0.0065 \times 1.85$
R _{glob} ($\text{MJ m}^{-2} \text{h}^{-1}$)*	Hourly	-
RH (%)*		
Validation data Data used in the comparison		
F _t ($\mu\text{g N m}^{-2} \text{s}^{-1}$)	Various (2-10 hourly)	Measurements in the midpoints of the collection periods were considered as representative hourly averages.
θ ($\text{m}^3 \text{m}^{-3}$)		

pH	Various	Measurements in the given hour
NH _x -N (μg N (g soil) ⁻¹)	(2-19 hourly)	were considered as representative hourly averages.

- 1 *From the National Climate Database for New Zealand (NIWA, 2015), all the other parameters
- 2 were measured at the site.
- 3

1 ~~Table 3. Model validation statistics~~4. Statistics calculated for the comparison of the modelled
 2 ~~and measured variables:~~ root mean square error (RMSE), ~~Pearson's correlation coefficient (r),~~
 3 ~~the equation of the fitted least-squares equation (x - observation, y - model)~~ and the level of
 4 significance of the correlation.

Variable*	RMSE	Equation	r	Level of significance
Ammonia emission flux	43.06 $\mu\text{g N m}^{-2}\text{g}^{-1}$	$y=34.63+0.50x$	0.54	0.01
Soil pH	0.56	$y=3.04+0.64x$	0.75	0.001
Model TAN budget vs. measured soil $\text{NH}_x\text{-N}$	-	-	0.63	0.01
Soil Volumetric water content	0.05 $\text{m}^3 \text{m}^{-3}$	$y=0.10+0.67x$	0.92	0.001

Formatted Table

Formatted: Left

5
6

1 Table 4.* All the modelled and measured variables are the same as shown in Fig. 4. In the case
2 of the emission flux, we compared the measured flux in the given measurement period with the
3 value simulated at the time of the midpoint of the corresponding measurement period as
4 explained in Table 2.

1 **Table 5.** The percentage of the change in total emitted NH₃ compared to the original run after
 2 modifying the different model constants by -20, -10, +10 and +20%.

Module	Parameters	Total NH ₃ emission change in response to change if parameter by			
		-20%	-10%	+10%	+20%
2LCCPM	z_1 (height of the top of logarithmic wind profile)	+0.02%	+0.01%	-0.01%	-0.02%
TAN budget	Δz (thickness of NH ₃ emission layer)	-11.7%	-5.57%	+5.07%	+10.5%
	A_{patch} (area of a urine patch)	+1.39%	+0.67%	-0.58%	-1.61%
Soil pH	β (soil buffering capacity)	+1.29%	+0.64%	-0.62%	-1.22%
Water budget	REW (readily evaporable water)	-2.98%	-1.69%	+2.06%	+4.32%
	θ_{fc} (field capacity)	-18.4%	-6.63%	+6.34%	+9.12%
	Θ_{pwp} (permanent wilting point)	+9.48%	+4.60%	-4.42%	-8.85%

3

4

1 Table 5-6. The results of the sensitivity analysis to the different meteorological variables. We
 2 changed these by $\pm \Delta x$ derived based on the minimum and the maximum of the given parameter
 3 over the modelling period ($\Delta x = (\text{Max}-\text{Min})/10$), and calculated the difference in the total
 4 emission over the modelling period compared to the original run. We also calculated the
 5 correlation (r) between the original input variables and the modelled hourly NH_3 emission
 6 fluxes.

Variable	Min	Max	Δx	Total NH_3 emission change in response to change in parameter by		r
				$-\Delta x$	$+\Delta x$	
u (ms^{-1})	0.62	8.59	0.80	-5.5%	+4.7%	0.40
T_{soil} ($^{\circ}\text{C}$)	11.6	27.9	1.64	-2.6%	+2.7%	0.58
p (kPa)	99.9	102.3	0.24	+0.0%	-0.0%	-0.33
T_{air} ($^{\circ}\text{C}$)	13.5	29.0	1.56	-2.4%	2.9%	0.60
R_{glob} ($\text{MJ m}^2 \text{h}^{-1}$) ^a	0.00	3.32	0.33	-2.0%	+4.1%	0.32
RH (%) ^b	30	95	6.50	+9.1%	-8.6%	-0.49
RH (%) ^b	only for evaporation ^c			+3.2%	-2.8%	-
P (mm) ^d	0.00	0.83	0.08	-0.7%	+0.8%	-
T_{air} and T_{soil} ($^{\circ}\text{C}$)	-	-	-	-4.9%	+5.7%	-

7 ^aWhen changed by $-\Delta x$, negative values were replaced by 0.

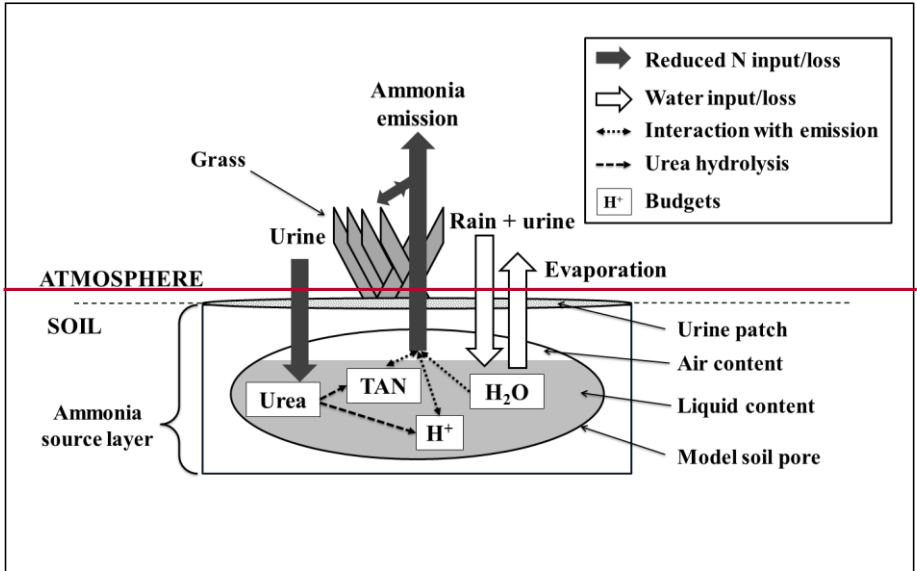
8 ^bWhen changed by $+\Delta x$, values greater than 100% were reduced to 100%.

9 ^cIn this test RH was modified by the same extent but only in the evaporation module.

10 ^dThe hourly precipitation sum was changed only in the hours when there was precipitation
 11 originally.

12

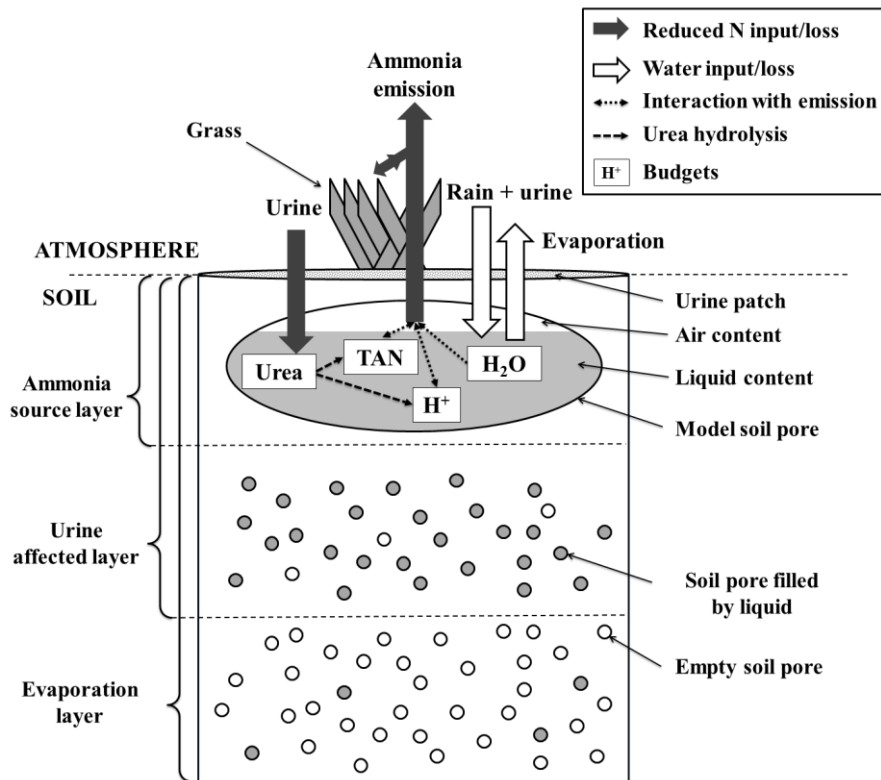
Formatted: Space After: 8 pt, Line spacing: Multiple 1.08 li



1
 2 Table 7: Comparison of the total emission (g N) from a single urine patch from the model runs
 3 assuming different N content of the urine deposited with the original temperature and +10°C
 4 (both in air and the soil temperature) scenario. We also calculated Q₁₀ as the ratio of the total
 5 emission for the original and the amended temperature scenario.

	<u>Total emission (g N)</u>		
	<u>Original</u>	<u>+10 °C</u>	<u>Q₁₀</u>
<u>Base run</u>	<u>95.8</u>	<u>121.0</u>	<u>1.26</u>
<u>3x N content</u>	<u>290.4</u>	<u>370.8</u>	<u>1.28</u>
<u>5x N content</u>	<u>489.7</u>	<u>613.8</u>	<u>1.25</u>

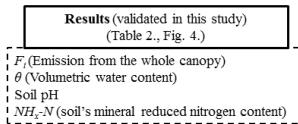
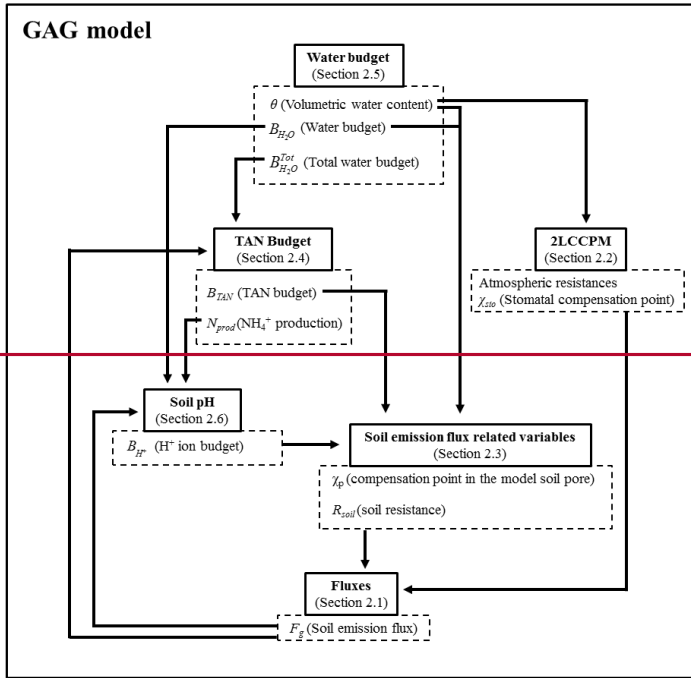
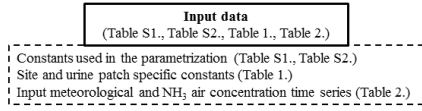
6
 7

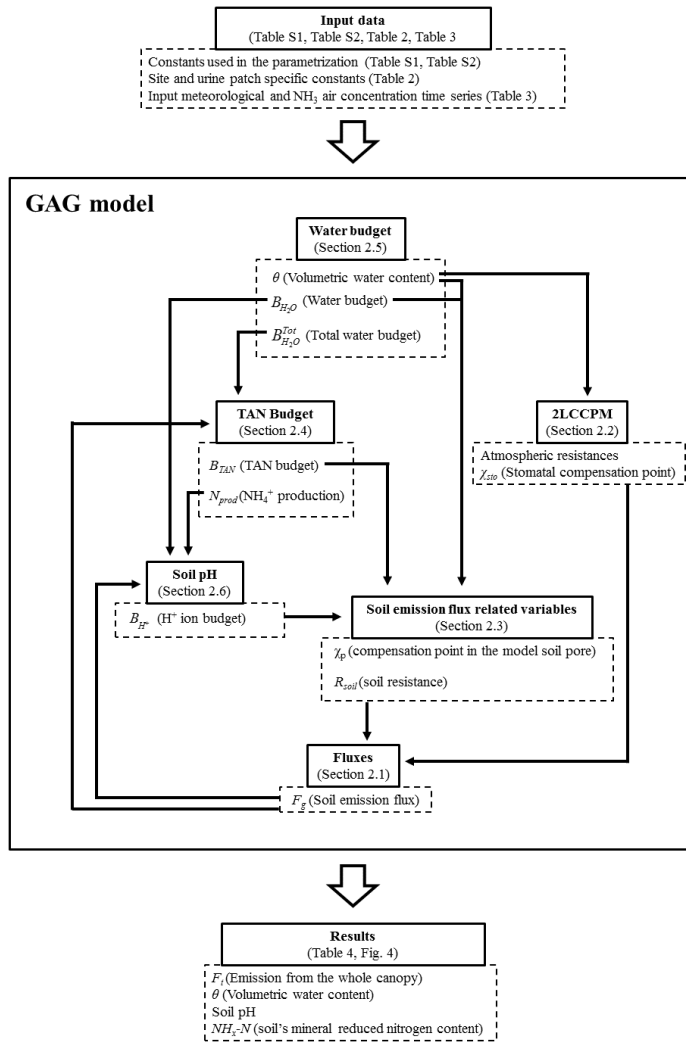


1

2

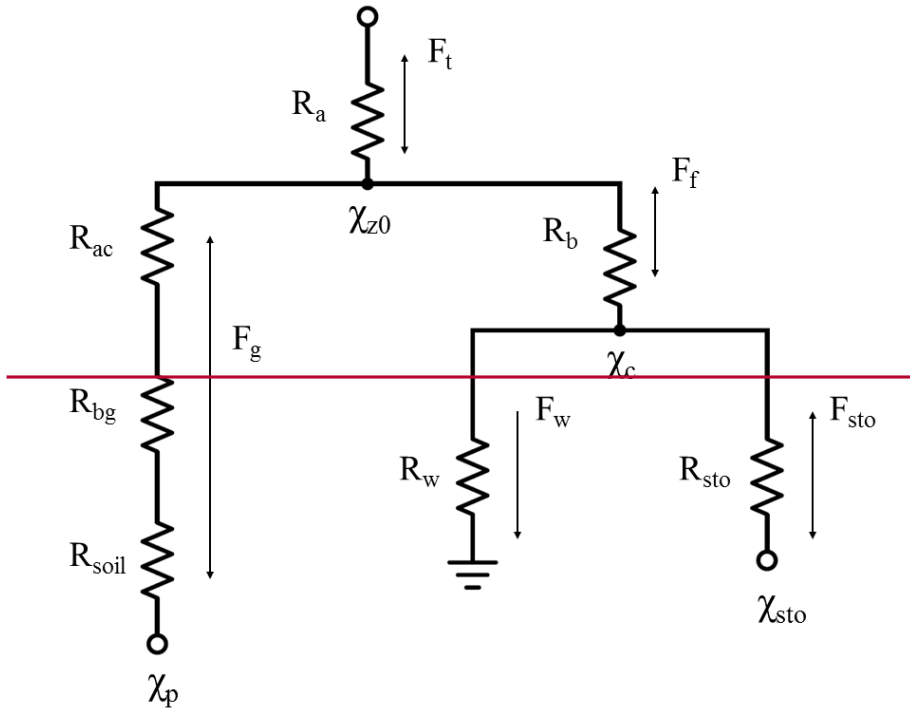
3 Figure 1. Schematic of major relationships in the GAG model. Empty soil pores in the middle
 4 layer represents that the maximum water content in the model is field capacity instead of being
 5 saturated. Whilst in the bottom layer the soil pores filled by liquid represents that the lowest
 6 water content is at the permanent wilting point instead of being completely dry. For more details
 7 on schematic see the text of Section 2.



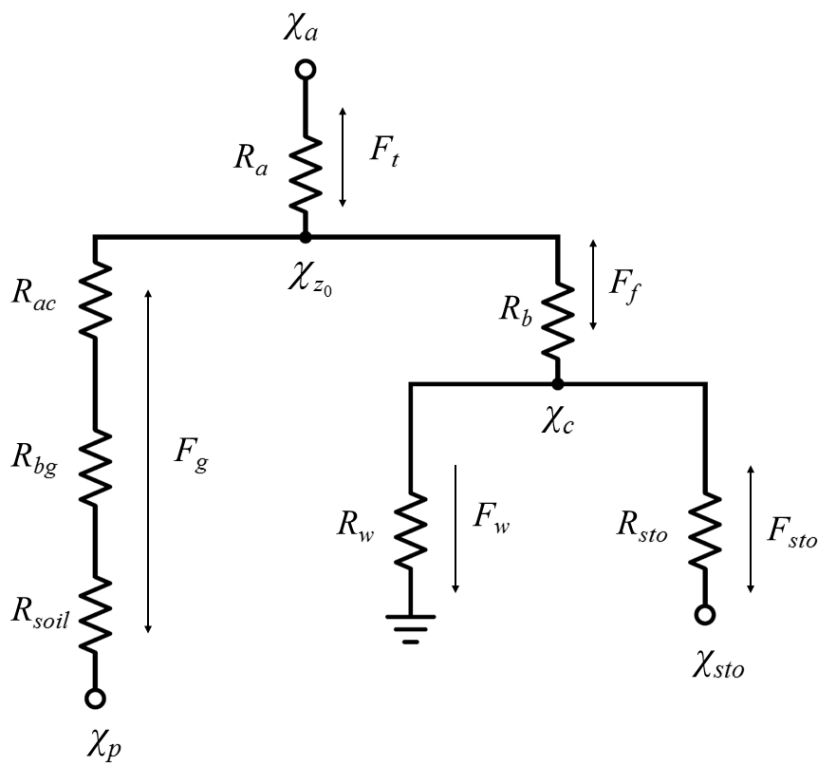


1
2
3 Figure 2. A flowchart depicting the steps of the calculation in the GAG model (middle panel),
4 processing the input data (top panel) to the results that were validated compared with
5 measurements in this study (bottom panel). The figure indicates the key variables that are
6 carried from one module to another module(s). The figure, table and section numbers referred

- 1 in the figure show where further description of the different model parts can be found in this
- 2 paper. (2LCCPM stands for Two-Layer Canopy Compensation Point Model.)



3

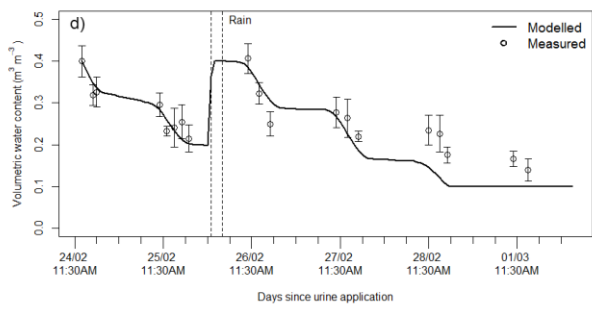
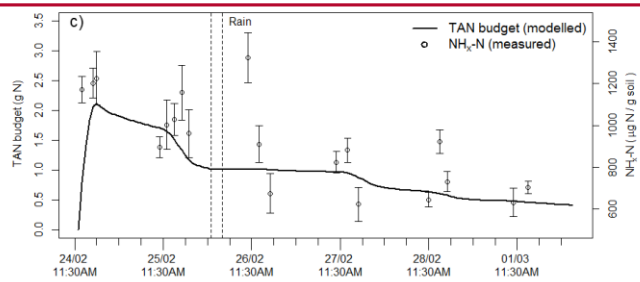
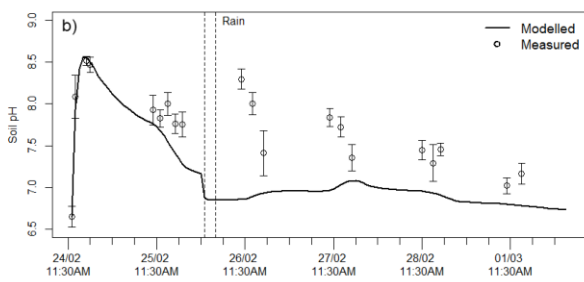
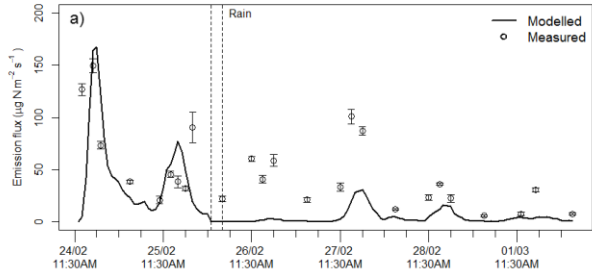


1

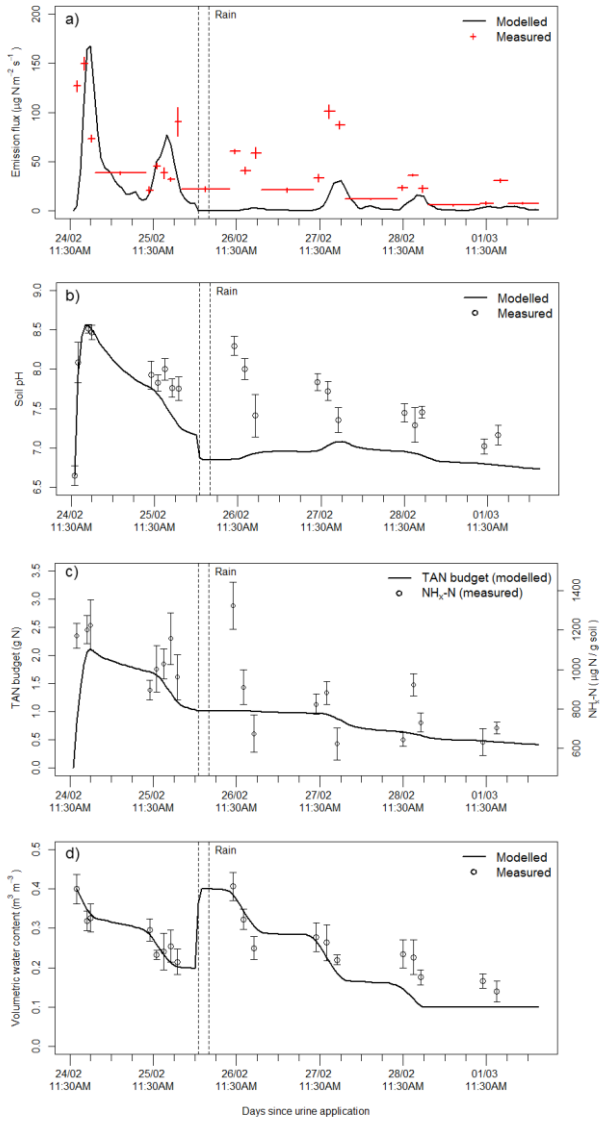
2

3 Figure 3. The network of gaseous resistances (R), ammonia concentrations (χ) and ammonia
 4 fluxes (F) used in the GAG model, which is based on the two-layer canopy compensation point
 5 model of Nemitz et al. (2001) incorporating concentration of the soil pore (χ_p) and soil
 6 resistance (R_{soil}). For the description of the other parameters in the framework see the text of
 7 this section.

8



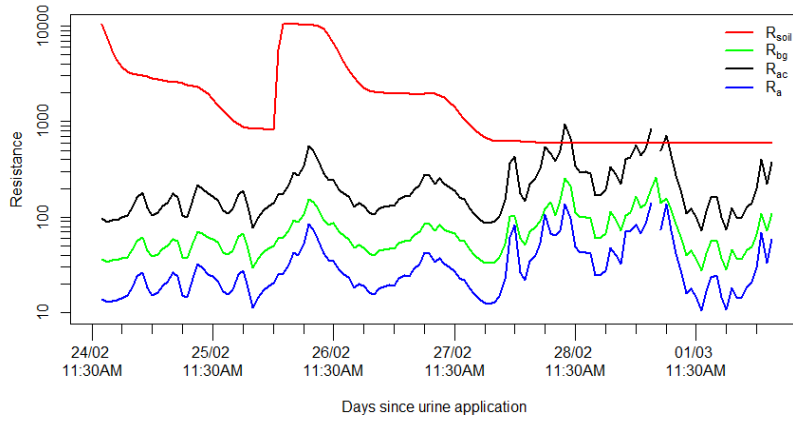
1



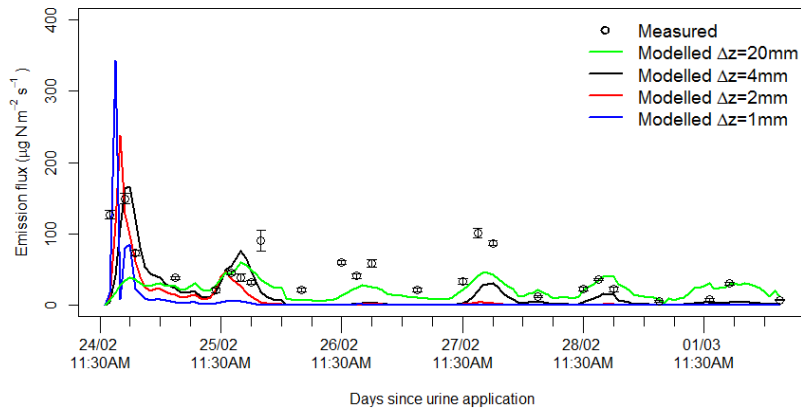
1
2
3 Figure 4. Comparison of modelled and measured values for NH_3 emission flux with the
4 corresponding sampling periods of the measurements (a), soil pH (b), TAN budget and $\text{NH}_4\text{-N}$

Formatted: Subscript

1 (c), and volumetric water content of the top 5 mm layer of the soil (d). The vertical error bars
2 stand for the standard deviation in the measurements.
3



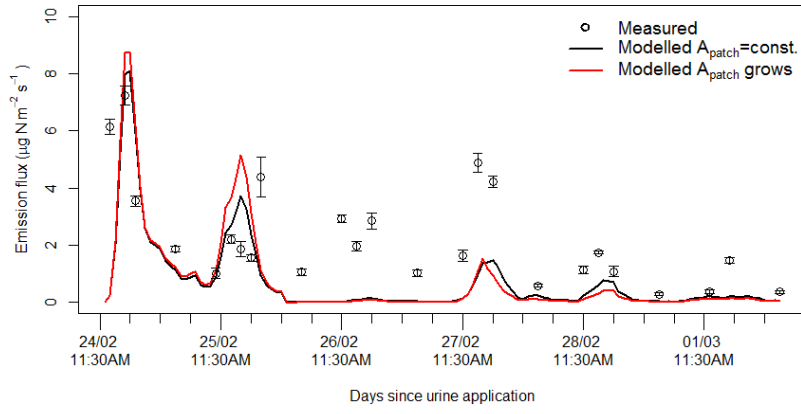
1
 2
 3 Figure 5. The atmospheric and the soil resistances over the modelling period. (At the time of
 4 the missing values in R_{bg} , R_{ac} and R_a u^* was 0, for which resistances are infinite. In these cases
 5 emission flux was assumed to be 0.)
 6



1
2
3
4

Figure 6. NH₃ fluxes from a urine patch with different Δz values.

1

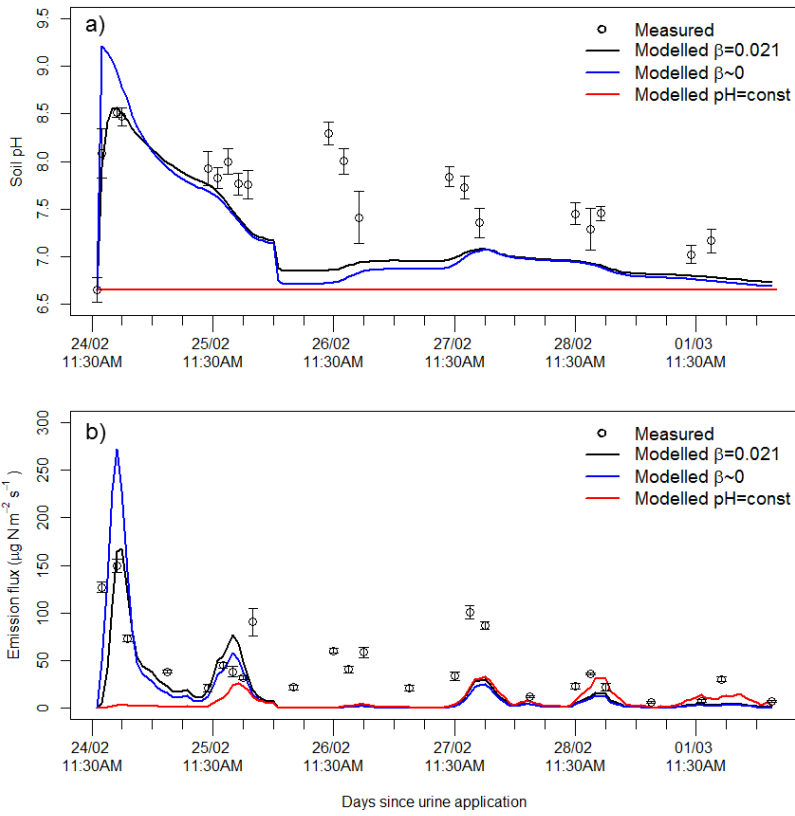


2

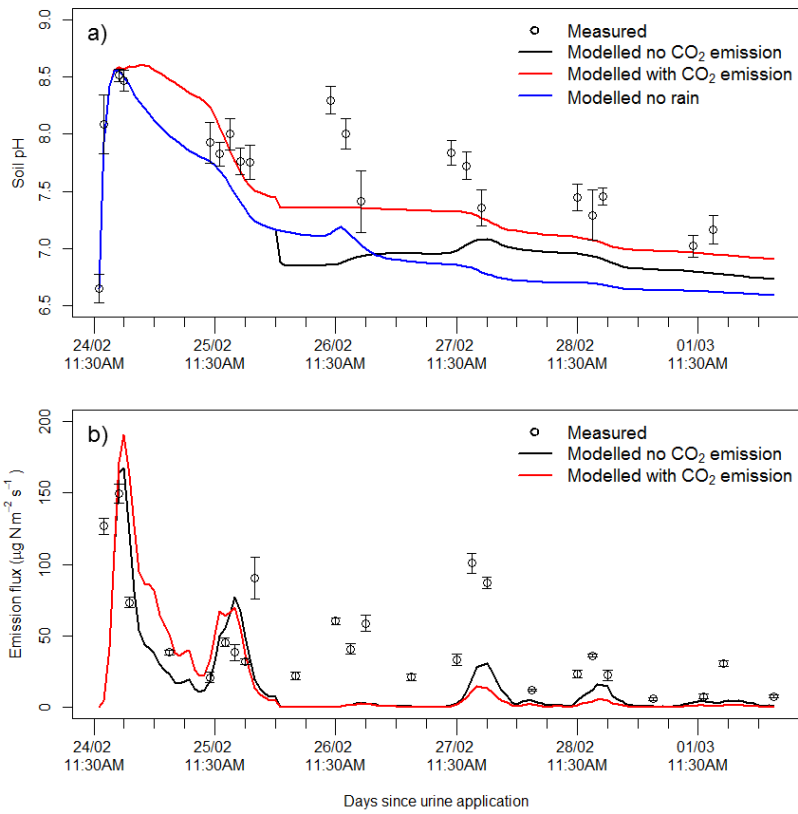
3

4 Figure 7. NH_3 fluxes from the whole experimental area with constant and with gradually
5 growing urine patches.

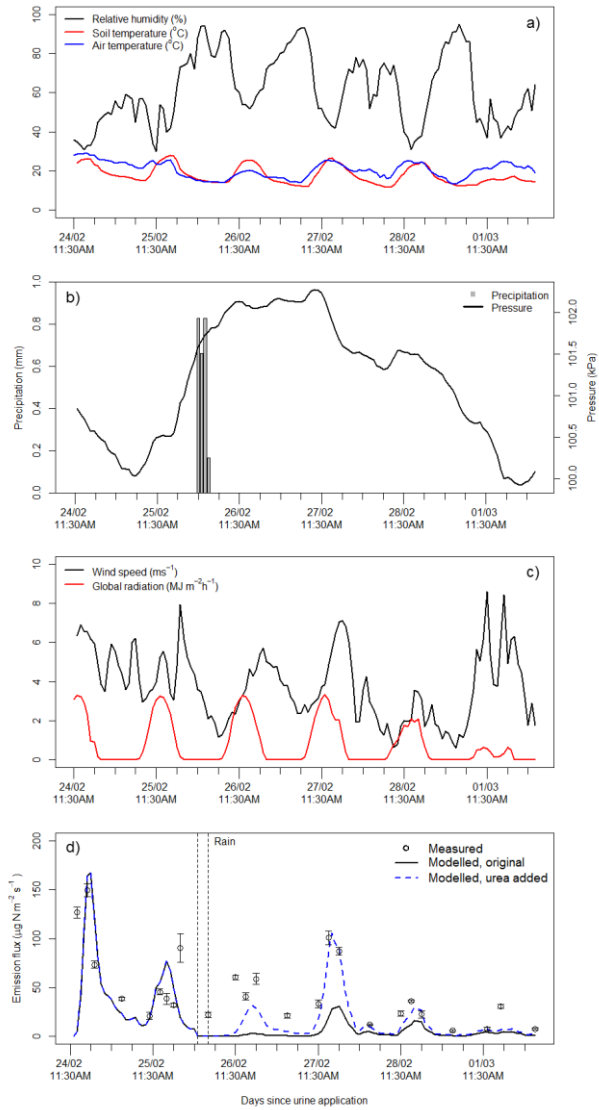
6



1
 2
 3 Figure 8. Soil pH under a urine patch (a) and NH₃ emission from it (b) with the currently applied
 4 buffering capacity ($\beta = 0.021$, original run), with no buffering ($\beta = 0$) and with constant pH,
 5 together with the measured values.
 6



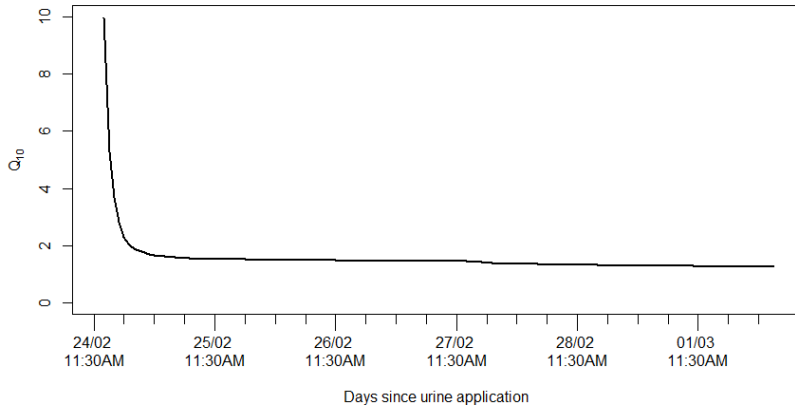
1
 2
 3 Figure 9. Soil pH under a urine patch (a) and NH₃ emission from it (b) without CO₂ emission
 4 (original run) and with an assumed CO₂ emission. On panel a) the original run without rain is
 5 also plotted.
 6



1
 2
 3 Figure 10. The investigated meteorological variables (relative humidity, soil and air
 4 temperature (a), precipitation and surface pressure (b), wind speed and global radiation (c)) and
 5 the hourly NH_3 fluxes (d) simulated by the original model (black line) and the modified model

1 (dashed blue line), in which fresh urea was assumed to washed into the soil during the rain
2 event.

3



1 _____
2 Figure 11. Calculated Q_{10} values for the cumulative NH_3 emissions between urine application
3 and the given time step.

Formatted: English (United Kingdom)